F_W from Equation 21 and $(LF)_W$ from Equation 12 may be substituted into Equation 17 to arrive at the following for C bedding (1 lbf = 0.004 kN):

$$(LF)_V = (2101/F_V) + 0.81; F_V(lbf/ft) \quad (22)$$

Similarly, F_W from Equation 21 and $(LF)_W$ from Equation 13 can be substituted into Equation 17. The result is the following equation for B bedding (1 lbf = 0.004 kN):

$$(LF)_V = (518/F_V) + 1.39; F_V(lbf/ft) \quad (23)$$

REFERENCES

1. M.G. Spangler and R.L. Handy. Soil Engineering, 3rd ed. Intext Educational Publishers, New York, 1973.
2. Design and Construction of Sanitary and Storm Sewers. In ASCE Manual and Report on Engineering Practice No. 37 (WPCF Manual of Practice No. 9), American Society of Civil Engineers and Water Pollution Control Federation, New York, 1973, pp. 210-211.
3. S.P. Timoshenko and J.N. Goodier. Theory of Elasticity, 3rd ed. McGraw-Hill, New York, 1970.
4. R.K. Watkins. A.P. Moser, and O.K. Shupe. Soil Supported Strength of Buried Asbestos Cement Pipe. Buried Structure Laboratory, Utah State Univ., Logan, 1976.

Publication of this paper sponsored by Committee on Culverts and Hydraulic Structures.

Rigid Pipe Prooftesting Under Excess Overfills with Varying Backfill Parameters

RAYMOND E. DAVIS AND FRANK M. SEMANS

Field testing and analyses of two culverts at Cross Canyon are described: a 96-in prestressed-concrete functioning culvert under 200 ft of overfill and an 84-in reinforced-concrete dummy culvert under a maximum 183-ft overfill in the same embankment. Eight instrumented and two noninstrumented zones in the dummy pipe and functional and unstressed control instrumented zones of the prestressed pipe were monitored during and after embankment construction to determine peripheral soil stresses, internal forces, and displacements. Correlations were established between quasi-theoretical and measured parameters (moments, thrusts, displacements, distress, etc.) with a programmed analysis. Some standard analytical tools (settlement ratio, finite element) were checked against observations, and relative costs of different construction modes were considered. Heger's recently developed criteria were checked against actual appearances of two of four distress modes. The programmed analysis was modified to predict these distress modes. Profiles of effective-density coefficients were established for various construction modes. The importance of designing for density distributions representative of contemplated construction modes is emphasized.

A comprehensive 15-year research program pertinent to structural behavior of culverts embedded in deep embankments (100+ ft) conducted by the California Department of Transportation (Caltrans) Structures Design Research Unit has been described (1-25). Eight papers (8,12,13,15-17,19,20) have discussed field tests of two reinforced-concrete pipe culverts at Mountainhouse Creek: a grossly underdesigned 1000D 84-in-diameter dummy culvert and (17) a functional 4000D 96-in-diameter pipe. Each pipe included six zones to be subjected to varying bedding and backfilling parameters. Buried under a 137-ft overfill (almost nine times the 16-ft maximum stipulated by current specifications), several zones of the dummy culvert responded encouragingly to specialized embedment techniques.

Tests of additional bedding and backfill parameters and pipe segments of varying strengths were conducted at Cross Canyon, near Sunland, California, to establish more realistic functional relationships between pipe strengths and allowable limiting overfills. Again, a functional culvert and a dummy pipe were tested.

Designed for 200 ft of overfill, the functional culvert is of 96-in diameter and 23.5-in wall thickness with two layers of closely spaced prestressing wires. Tests of one pipe segment (Zone 11) are described later.

The 84-in-diameter dummy culvert, its invert located 13 ft above the crown of the functional culvert at varying horizontal distances therefrom, was divided into 10 zones (Figure 1); pipe strengths and bedding and backfill parameters are as shown in Figures 2 and 3. Dummy pipe segments except those in Zones 5 (1750D), 6 (2500D), and 7 (3600D) were nominally classified as having a 1000D load rating; measured load ratings, based on tests of three pipe segments of each pipe strength, were Zones 1-4 and 8-10, 997D; Zone 5, 1910D; Zone 6, 2574D; and Zone 7, 3780D.

In all instrumented zones except Zone 1, at least one 8-ft-long pipe segment was placed on either side of the instrumented segment as a buffer segment where Method-A (ordinary embankment material) backfill was employed. Two segments were used in the zones (8, 9, and 10) with Method-B (low-modulus inclusion) backfill.

DESCRIPTION OF INSTRUMENTATION

Dummy culvert instrumentation design was influenced by observed behavior of culverts and instrumentation in earlier projects, briefly described as follows (Figures 4 and 5):

1. Symmetry of soil stress distribution has never been observed in Caltrans culvert research.
2. Integrated forces acting on pipe peripheries, based on measured soil stresses, have indicated vertical force unbalance often measured in tens of kips.
3. Failures of interface stress meters in sensitive locations or inconsistencies in measured stresses due to soil heterogeneity have often greatly decreased confidence in overall results.

Figure 1. Longitudinal section of dummy culvert showing zone divisions and overfills.

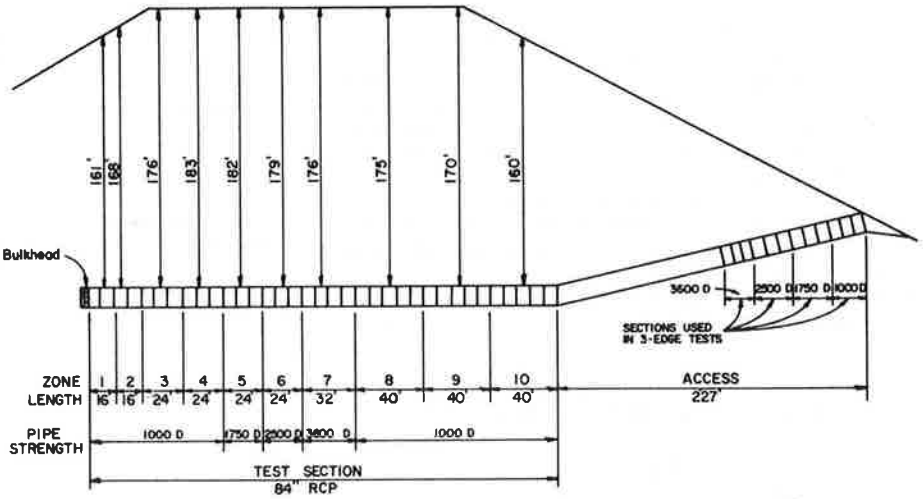

Figure 2. Bedding and backfilling parameters for Zones 1-7.

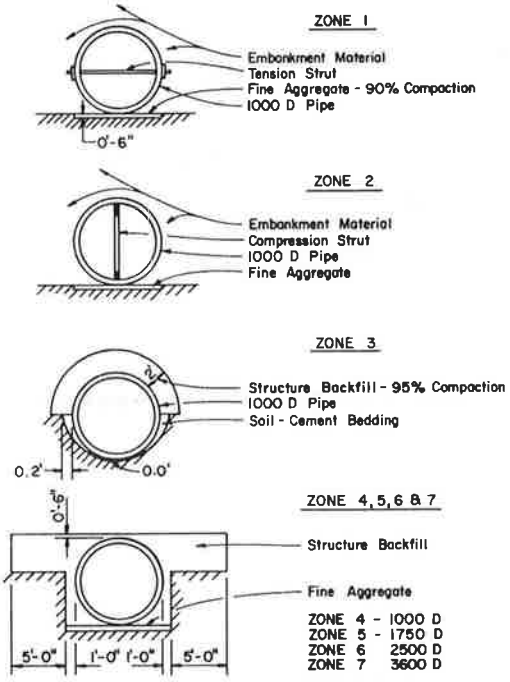

Figure 3. Bedding and backfilling parameters for Zones 8-11.

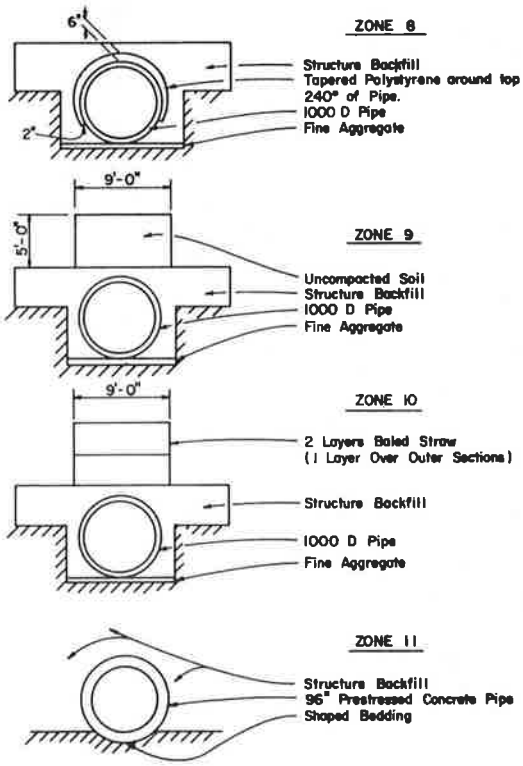

4. Lacking facility for measurement of tangential shear stresses acting at soil-concrete interfaces, researchers attributed deficiencies in static checks thereto.

Recently developed computer codes, Specifications of the American Association of State Highway and Transportation Officials (AASHTO) for effective-density distributions, and Marston-Spangler theories assume or produce soil stress distributions symmetrical about a conduit's vertical central plane. Observed asymmetrical loadings can produce significantly different structural behavior.

To detect asymmetry of loading and improve accuracy of force integrations, the researchers installed a heavy network of stress meters on both sides of the pipe (see Figure 5). Based on Hadala's recommendations (26), each zone was instrumented with three planes of stress meters at 3-ft spacing longitudinally, except Zones 1 and 9 (two planes) and Zones 2 and 7 (not instrumented).

Previous indications of static unbalance dictated need for a unique soil stress meter capable of measuring tangential forces. One complete plane of the three planes in each of Zones 4, 6, and 10 included 10 such Cambridge meters. [For comprehensive descriptions of soil stress meters, relative behavior, etc., see Caltrans report by Davis and others (24, Section 1, Vol. 1; Section 2, Vols. 1 and 2) and report by Jackura (27).]

Steel spheres affixed to the inner pipe wall at the octant points permitted measurements of shape changes. Fluid settlement platforms and Ormond and Kyowa stress meters were placed in the embankment at locations shown in Figure 6. Levels on monuments on

the pipe invert permitted assessment of pipe settlements and, in conjunction with fluid settlement platform measurements, of settlement ratios. Readings of an elevation rod placed on steel spheres near the springing lines indicated rigid body pipe rotations. Plate-and-rod settlement platforms were placed at outer surfaces of polystyrene planks at Zone 8 and at upper and lower surfaces of the uncompacted-soil and baled-straw layers in Zones 9 and 10. Differences in rod protrusions through holes cast in the pipe wall provided strain data for calculations of moduli of soft inclusions.

Figure 7 presents profiles of unadjusted soil stress increments for individual instrumented planes at Zone 3 at the 80-ft overfill based on a zero datum when the embankment was at crown level. Typically, some readings display wide divergence from those in similar locations in adjacent planes, but the majority exhibit reasonable comparisons.

Figure 4. Internal instrumentation of Cross Canyon culverts.

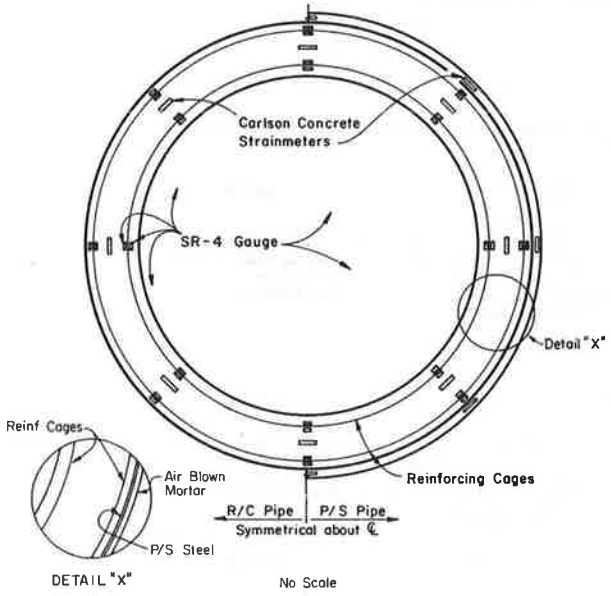

Figure 5. Soil stress-meter layout and instrumentation planes.

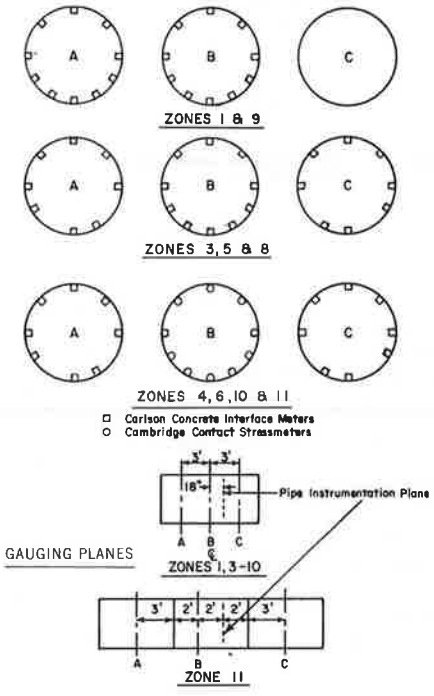

Figure 6. Locations of fluid settlement platforms, embankment soil stress meters, and plate-and-rod settlement platforms.

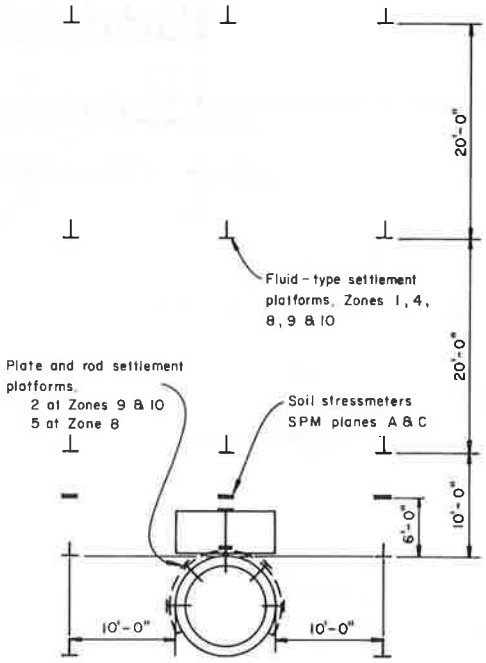

Figure 7. Profiles of unadjusted measured soil stresses at 80-ft overfill level, Zone 3.

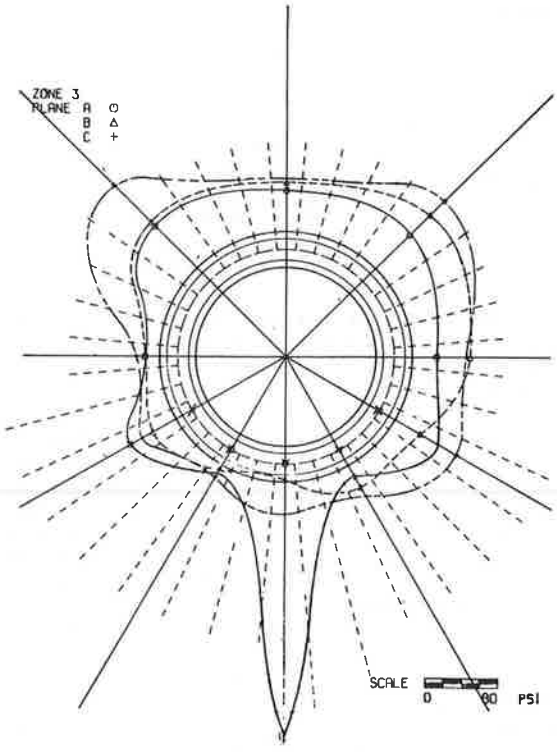

NEUTRAL-POINT ANALYSIS

Observed soil stress fields were used in conjunction with a programmed analysis based on the neutral-point method (24, Section 5, Vols. 1-12) to establish quasi-theoretical values of certain parameters for comparison with experimental values calculated from observed strain patterns, extensometer readings, visual observations, etc. Lacking static equilibrium in external forces, the analysis will produce large errors in calculated parameters.

The addition of Cambridge meters at Cross Canyon did not solve the problem of static unbalance, and it became necessary to induce static equilibrium artificially. Horizontal static unbalance was invariably small, and slight adjustments of normal forces produced equilibrium in this direction. Vertical static balance required synthesizing of tangential forces. Rotational equilibrium was first established for Zones 4, 6, and 10, where a set of interpolated tangential forces had been established from Cambridge-meter readings. These interpolated forces were altered by constant percentages to produce net zero summations of rotational forces and were then augmented or reduced as required to alleviate deficiencies in summed vertical force components.

For each remaining zone, tangential forces were synthesized that were symmetrical about the vertical diameter to ensure rotational equilibrium with magnitudes established to produce a total vertical force component equal in magnitude, but of opposite sign, to the unbalance in the summed vertical components of the normal forces. Each combination of adjusted normal and adjusted or synthesized shearing forces was then tested by the neutral-point analysis for compatibility with internal pipe wall forces based on stress-meter readings and readjusted as required.

Traditionally, Caltrans researchers have normalized normal tractions by converting them into effective densities, i.e., embankment densities required under hydrostatic conditions to produce given measured values of soil stress increments ΔP under given overfill increments ΔH. Thus,

$$\text{Effective density (pcf)} = 144\Delta P \text{ (psi)}/\Delta H \text{ (ft)}.$$

Interpolated effective densities for Zones 1 and 3, based on the adjusted normal tractions, are shown in Figures 8 and 9. Since functions of soil stress and overfill are nonlinear, effective-density profiles vary with overfill. Profiles have been included for 20-ft, 80-ft, and 160-ft overfills to illustrate typical distributions for relatively low, mid-height, and deep overfills (by California standards); for maximum overfills (where they differ appreciably from 160 ft); and for 24 months after achieving maximum overfills to illustrate time dependency.

Adjusted normal and tangential forces were used in conjunction with neutral-point analyses and experimental parameters to derive information about pipe structural behavior and relative effects of various bedding and backfilling parameters on that behavior.

Figure 10 depicts quasi-theoretical (i.e., based on measured soil stresses and theoretical analyses) wall bending moments with superimposed experimental moments based on measured strain data; Figure 11, quasi-theoretical wall displacements with superimposed displacements based on extensometer measurements, with a datum at the inner pipe invert; Figure 12, quasi-theoretical concrete extreme fiber stresses, all for Zone 3; and Figures 13, 14, and 15, changes in horizontal and vertical diameters as functions of overfill.

In the plots of inner and outer concrete extreme fiber stresses, a circular line was added at a tensile stress of 400 psi, assumed to be the limiting tensile working stress for concrete. The intersections of this curve with that for quasi-theoretical inner fiber tensile stresses suggest boundaries of observed cracking. These limits are designated Q-T (quasi-theoretical) and O (observed).

Pipe behavior was evaluated in part on the basis of observed distress, e.g., total lengths and maximum widths of cracking, delamination (i.e., shell separation in circumferential reinforcement planes), and diameter changes. Distress in all pipe segments was assessed separately, but the most significance, in comparisons of behavior, was attached to central segments in each zone, most distant from adjacent zones. Based on total length of cracking as the most significant criterion for comparison, the following information may be derived.

Zone 1 (high-strength steel tensile struts, full projection) exhibited a relatively small amount of cracking up to 70 ft but dropped into fifth place at fill completion. The high-strength rods provided lateral support at least as good as that provided by entrenchment throughout the entire course of embankment construction, and total diameter changes after rod removal were less than those at entrenched Zone 7 at Mountainhouse Creek.

This test could not assess behavior for low overfills for this parametric condition, since lateral support must be provided before and after rod removal. It had been hypothesized by the researchers that the deep overburden would compact soil on the sides of the pipe sufficiently to provide significant passive components of soil stress on rod removal to furnish required support. Ample evidence bears out this hypothesis, since the increase in horizontal diameter 24 months after fill completion (0.952 in) (see Figure 13) was less than the 1 5/8-in increase at entrenched Zone 7, Mountainhouse Creek, Part 1, under about half the overfill, and only 11 percent of the increase at positive-projecting Zone 9, Mountainhouse Creek, Part 1. The same degree of compaction would probably not have been obtained at much lower overfills, and rod removal prior to achievement of this compaction would almost certainly have produced the same pronounced distress observed at Zone 9, Mountainhouse Creek, Part 1.

Measured effective densities acting laterally on the pipe increased, while those at the crown and invert decreased after rod removal as a result of increases in the horizontal diameter and development of passive components of soil stress and local arching accompanying decreases in vertical diameter. [The augmentation of densities, shown at the ends of the horizontal diameter up to fill completion (but not thereafter), was determined by calculating the horizontal diameter changes (by the neutral-point analysis) for the unstrutted pipe under the observed soil stresses, calculating the horizontal forces required to produce the measured displacements, and treating these forces as additional soil stresses acting on two elements on each side.]

The first 0.01-in crack was observed in Zone 1 with the overfill at 67 ft.

Throughout the entire course of embankment construction and for 24 months following embankment completion, Zone 2 (timber compression struts, full projection) consistently exhibited the greatest total length of cracking. Since vertical timber struts do not provide the very important lateral support for the fully projecting pipe, this type of construction is not conducive to good pipe behavior.

Hundredth-inch cracks were first observed in Segment 202 at 51 ft of overfill and in Segment 203 at

57 ft. Delamination was observed for the first time at an overfill of 122 ft and compression spalling at the springing line at 137 ft. At higher overfills, extensive crushing of timber sills and wedges above the vertical struts was observed. Diameter changes were 2.5 times as large vertically and 3.3 times as large horizontally as those in entrenched Zone 4. The behavior of Zone 1, which had tension struts, was markedly better than that of Zone 2, which had compression struts.

Figure 8. Effective-density profiles, Zone 1.

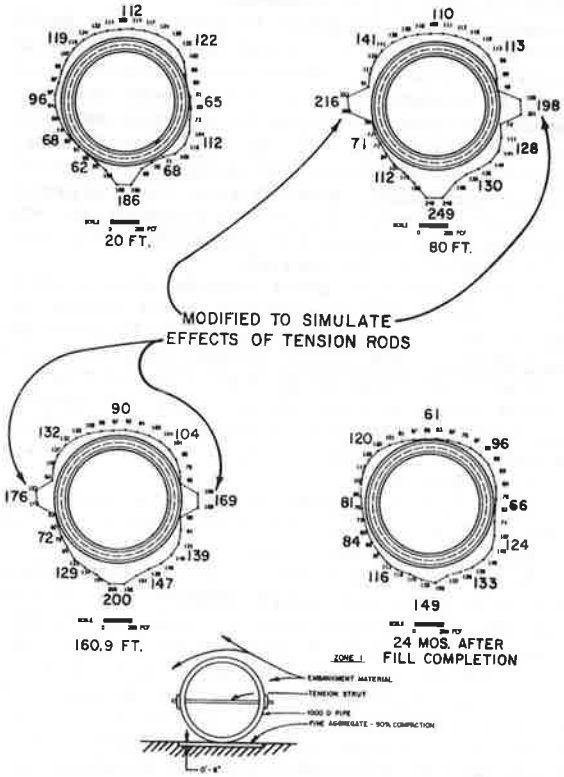

Figure 9. Effective-density profiles, Zone 3.

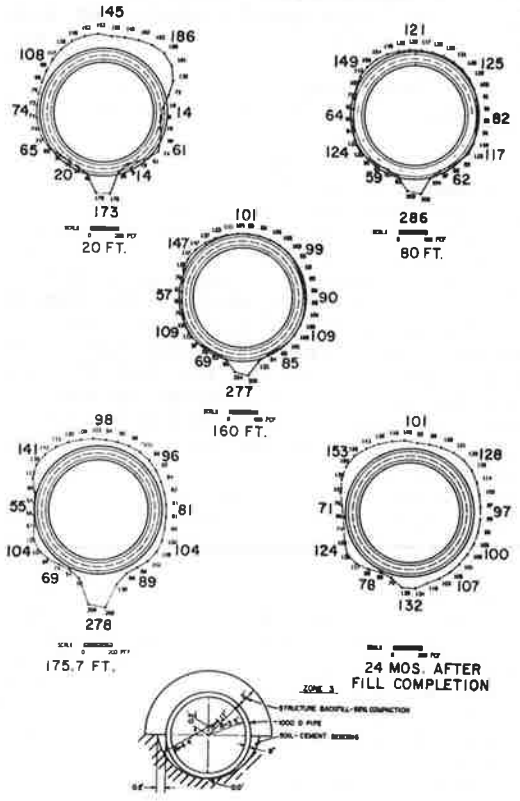

Figure 10. Quasi-theoretical bending moments with experimental moments, Zone 3.

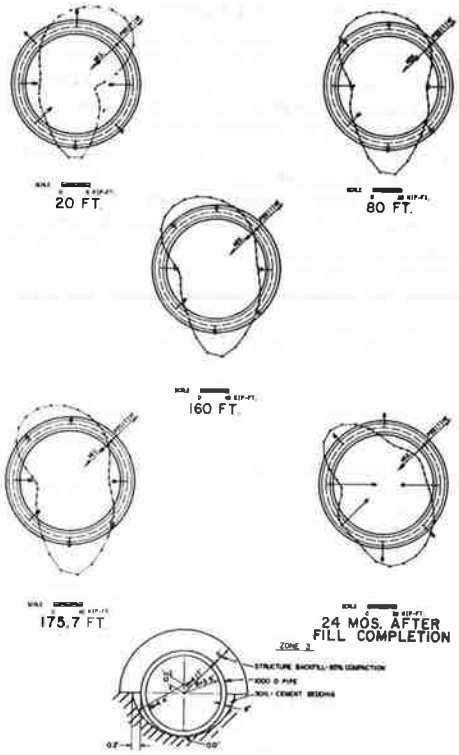

Figure 11. Quasi-theoretical pipe wall displacements with experimental displacements, Zone 3.

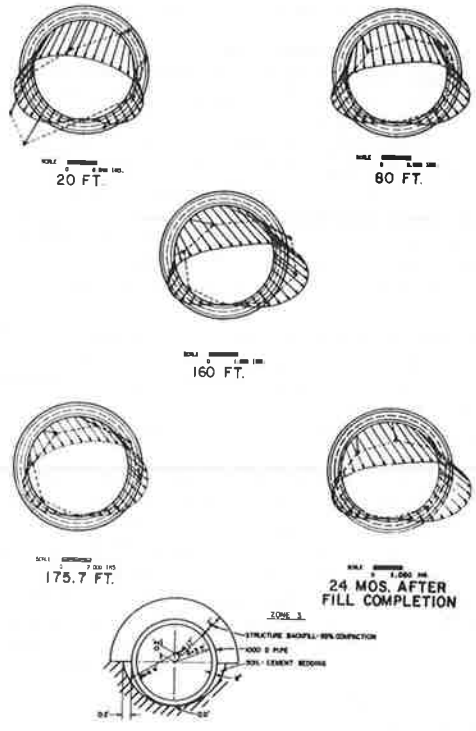

The Zone-3 construction method, extensively employed in the pipe industry, seems conducive to excellent structural behavior, since placement of the cement-soil slurry should eliminate irregularities of typical preshaped beddings and produce essentially uniform distributions of soil stress over the entire lower half of the pipe.

Surprisingly, then, Zone 3, from the viewpoint of total crack length, performed poorly by comparison with other zones, and performance of the lower half of the pipe was particularly bad. Throughout much of the embankment construction, at deeper overfills, this section ranked second only to Zone 2 in total crack length.

Initial input soil stress distributions, more or less uniform around the upper and lower halves of the pipe (the latter being of considerably less magnitude than the former), required inordinately large synthesized tangential forces to produce static equilibrium. Predicted cracking and other parameters output from neutral-point analyses did not agree with observations and corresponding experimental values, so input soil stresses were revised to give more weight to the large soil stress acting at the invert at Plane A (see Figure 7). The resulting correlations of quasi-theoretical and experimental parameters were thereby much improved (e.g., see Figures 10, 11, and 12), which suggests that the Plane-A invert soil stress could not safely be ignored and that the desired uniform distribution was not really obtained after all--this Plane-A invert stress had not actually been ignored previously, but a very tight stress gradient combined with an input scheme using stresses 5° on either side of the high stress with the averaging process including two low-gradient planes obscured it.

From the viewpoint of crack width rather than total length of cracking, this construction method did produce noticeable improvement in behavior. If the center segment only is considered representative, the 0.01-in crack was first observed at an overfill of 61 ft compared with 40 ft for adjoining Zone 4, which employed the unshaped fine-aggregate bedding. The 0.01-in crack for the 1000D pipe in Zone 3 thus appeared at the same overfill as that which may be considered representative for the entrenched 1750D (Zone 5) pipe with the fine-aggregate bedding (see Figure 33).

Diametral changes at comparable overfills in Zone 3 were of nearly the same magnitude as those in Zone

Figure 12. Quasi-theoretical concrete extreme fiber stresses, predicted zones of inner wall cracking, and limits of observed cracking, Zone 3.

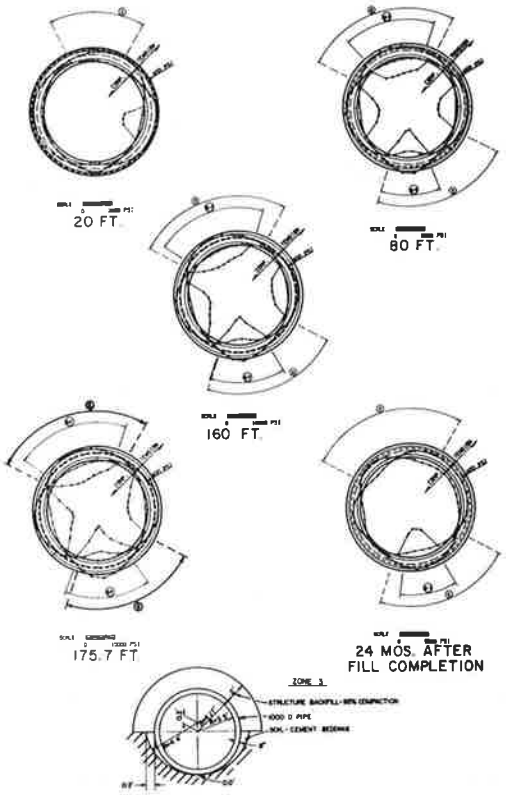

Figure 13. Changes in horizontal and vertical pipe diameters as function of overfill and time after embankment completion, Zone 1.

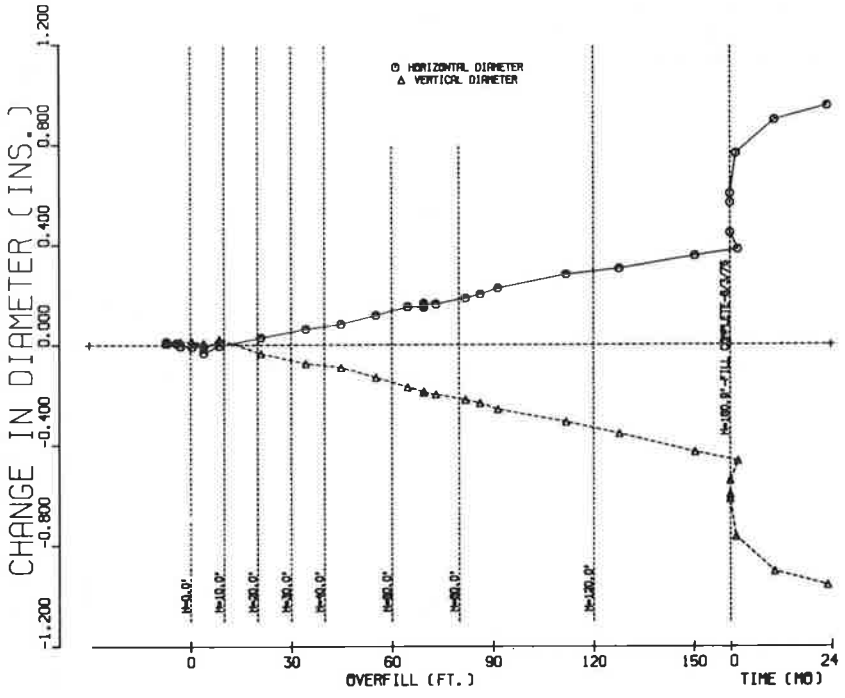

1 prior to removal of the steel rods, which proves that the lateral support provided by the trench and cement-treated slurry was almost as good as that provided by the tension struts. The soil stress distribution around the lower half of the pipe was better than at other zones in the centers of the lower quadrants, but a strong gradient of soil stress existed in the vicinity of the invert (see Figure 9). Behavior of the other zones will be described later.

OBSERVATIONS OF ENTRENCHED METHOD-A AND METHOD-B ZONES

Effective-density profiles are depicted for Zones 4, 5, 6, 8, 9, and 10 in Figures 16 through 21. These profiles exhibit a characteristic pattern: density maxima at upper quadrant midpoints and invert (1:30, 6:00, and 10:30 o'clock); density minima at the crown and lower quadrant midpoints (12:00, 4:30, and 7:30 o'clock). There were two exceptions: Zone 8 manifested a very uniform distribution about the upper 240° of the pipe periphery at and above the

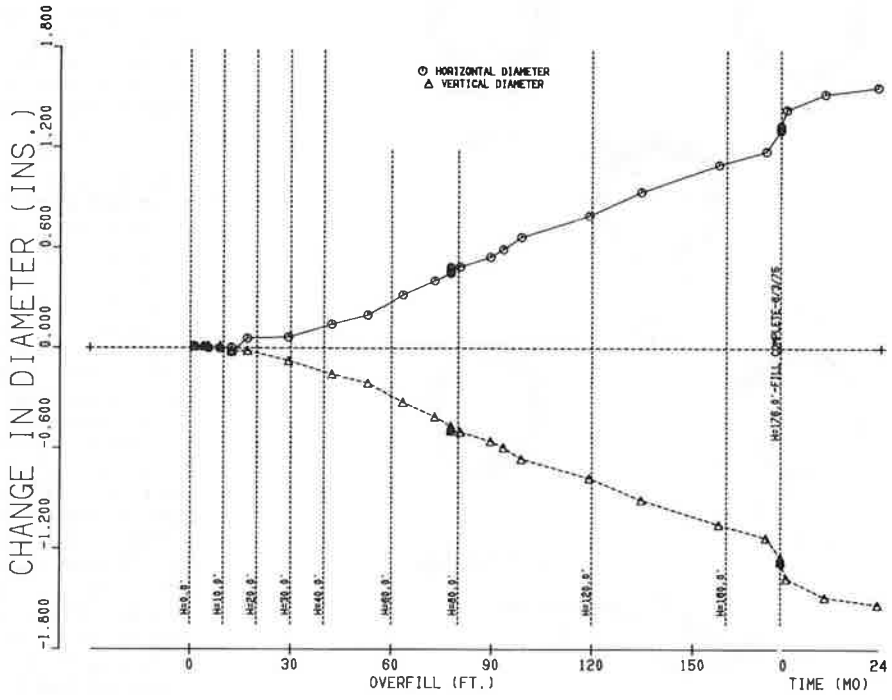

Figure 14. Changes in horizontal and vertical pipe diameters as function of overfill and time after embankment completion, Zone 2.

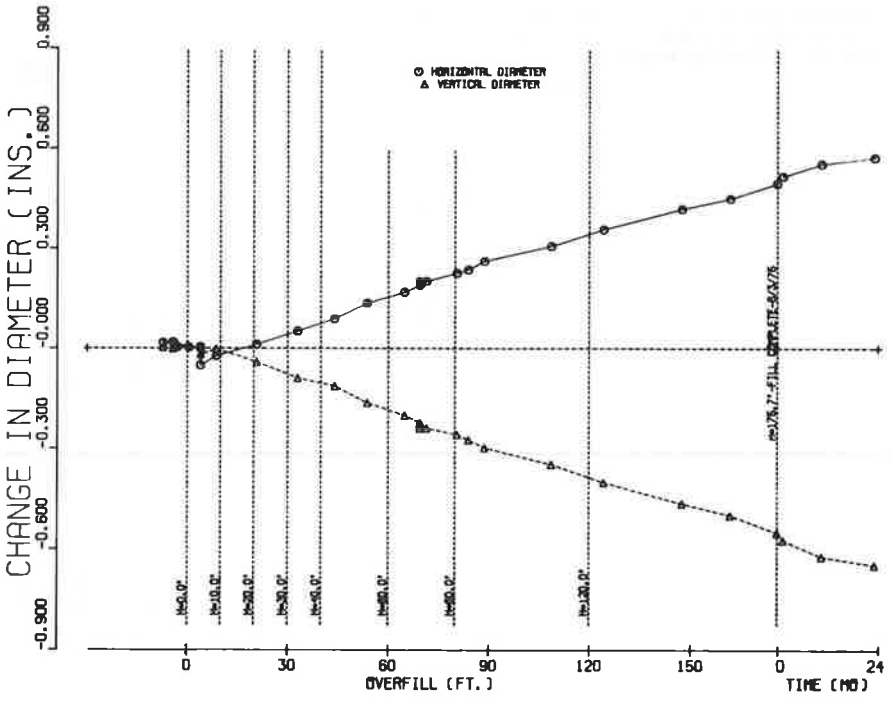

Figure 15. Changes in horizontal and vertical pipe diameters as function of overfill and time after embankment completion, Zone 3.

Figure 16. Effective-density profiles, Zone 4.

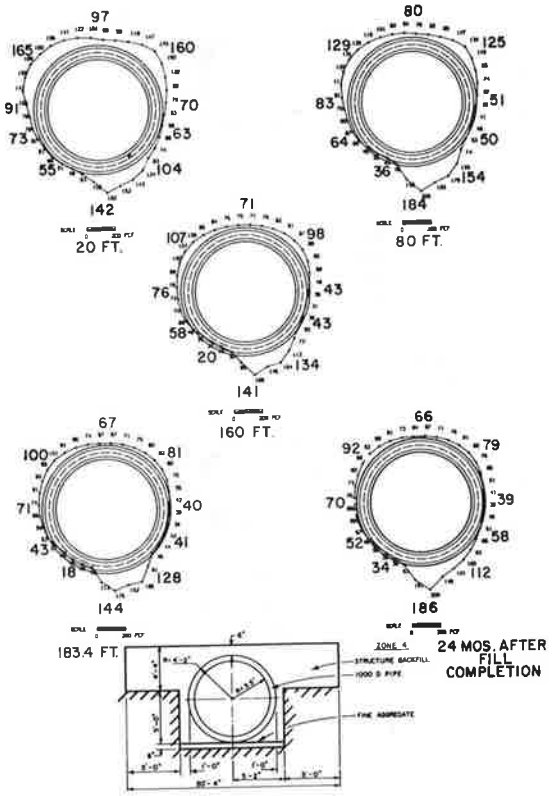

Figure 17. Effective-density profiles, Zone 5.

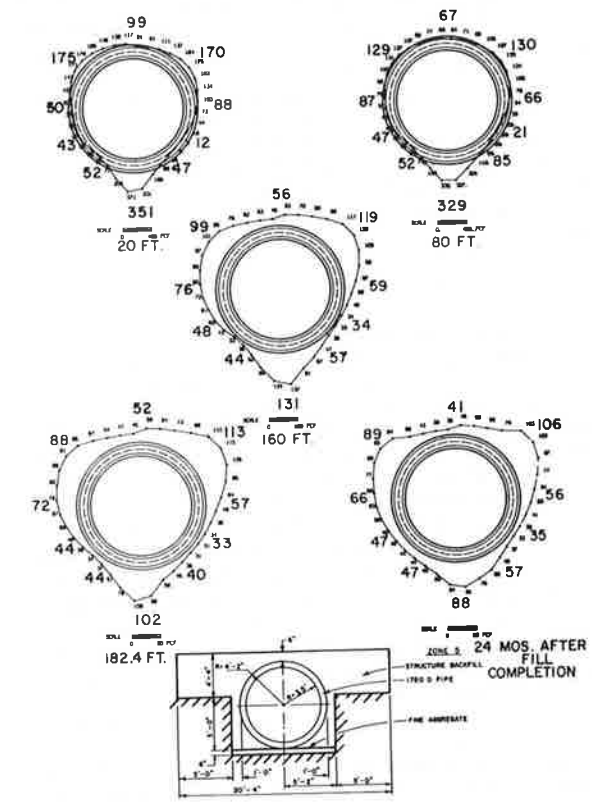

Figure 18. Effective-density profiles, Zone 6.

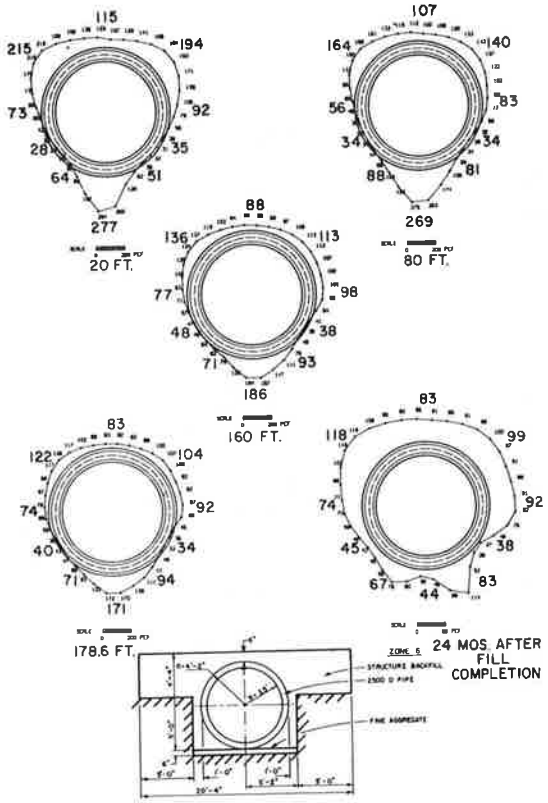

Figure 19. Effective-density profiles, Zone 8.

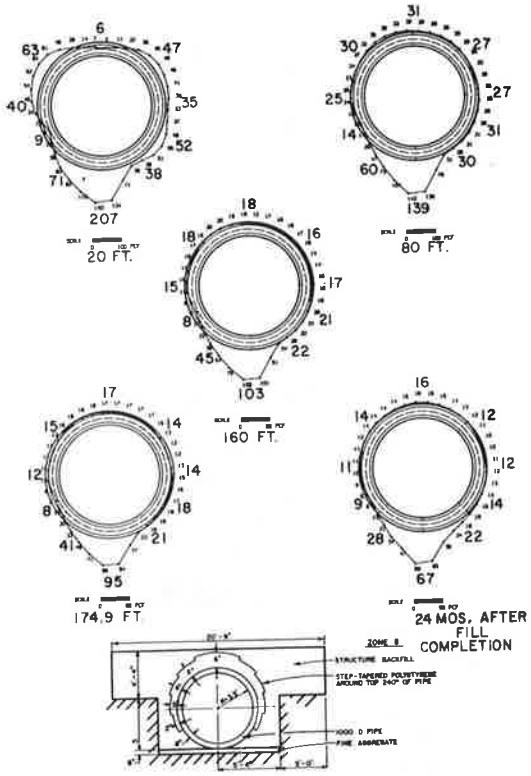

Figure 20. Effective-density profiles, Zone 9.

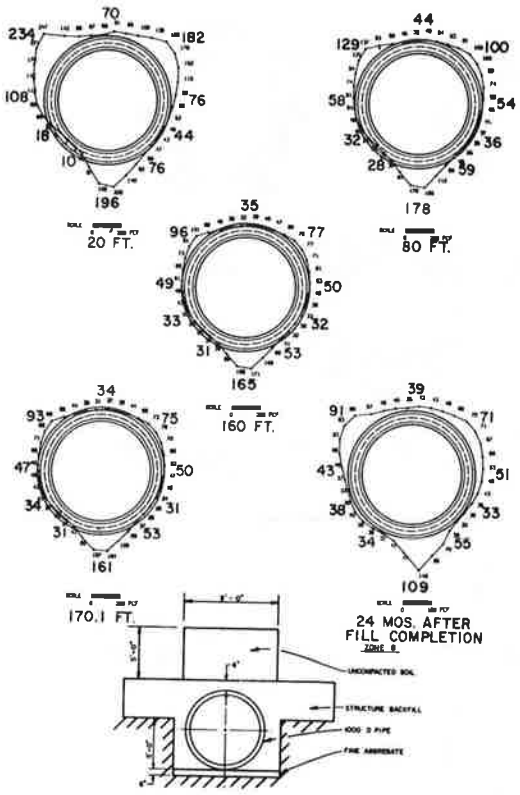

Figure 21. Effective-density profiles, Zone 10.

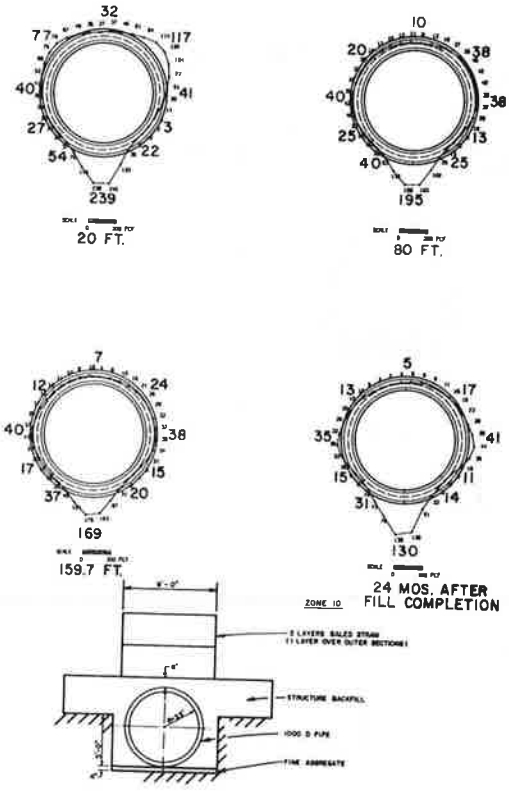

Figure 22. Quasi-theoretical pipe wall displacements compared with experimental displacement, Zone 4.

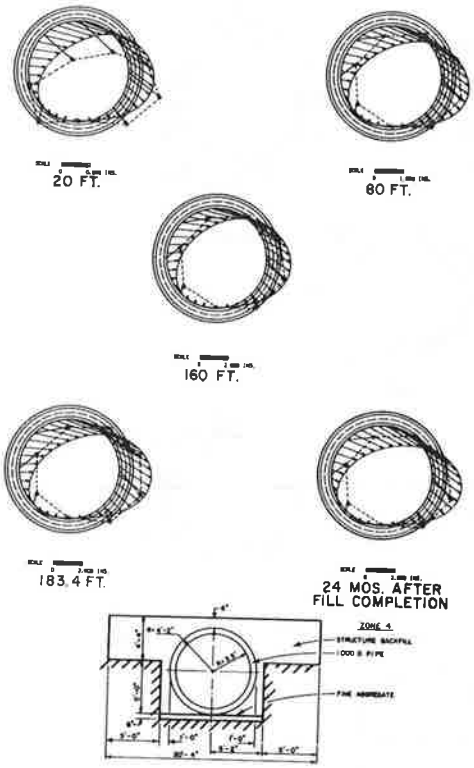

midlevel overfills and Zone-10 maxima moved from the upper quadrants to springing lines above midlevel overfills.

Nonlinear soil stress overfill functions produced general decreases in secant effective densities at the crown, upper quadrants, and invert, whereas lower quadrant densities tended to remain constant. Density maxima tended to decrease more rapidly than minima; there was a trend toward more uniform density distributions with increasing overfill.

Four zones (4, 5, 6, and 7) were placed in a stepped trench and bedded on a shallow layer of compacted fine aggregate (see Figure 2). Observations are described below.

Zone 4 (1000D Pipe)

Quasi-theoretical extreme fiber stress curves predicted limits of cracking with fair accuracy. Cracks appeared at lower overfills than at comparable Zone 8, Mountainhouse Creek, but did not develop to the same widths at higher overfills.

Measured wall displacements agreed favorably with quasi-theoretical ones (Figure 22), especially those based on Cambridge-meter stresses.

Diametral changes agreed closely with those in Zone 3 (cf. Figures 15 and 23), which demonstrates that 95 percent compacted structure backfill between pipe and trench can provide lateral support comparable with that of cement-treated backfill at the sides of the pipe. However, cement-treated backfill provides better support and more uniform soil stress gradients in lower quadrants (exclusive of the invert) where structure backfill is more difficult to consolidate by hand.

Diameter changes were much smaller at Zone 4 than at comparable Zone 8, Mountainhouse Creek (see Figure 23), even though installation procedures were supposed to be the same, which possibly indicates

differences in stringency of inspection, particularly in placement and compaction of structure backfill between the sides of the pipe and trench. Although this research will demonstrate feasibility of appreciable savings by use of lesser pipe strengths, it cannot be overemphasized that in order to take advantage of soil-structure interaction, suggested construction procedures must be performed under stringent inspection. For example, special consideration must be given to placement of backfill under lower pipe quadrants. California specifications recently increased the distance between pipe walls and sides of the trench from 1 ft to 2 ft to accommodate nuclear compaction testing equipment; this change will also help construction workers reach this relatively inaccessible area with hand-operated compaction tools.

Current California specifications prohibit placement of 1000D pipe in any highway embankment, and where this pipe strength is permitted, maximum allowable overfill is 16 ft. At Mountainhouse Creek, Part 1, entrenched 1000D pipe in Zones 7 and 8 did not exhibit hairline cracks until 44 ft of overfill had been placed. The plot in Figure 24 depicts overfills at which the 0.01-in crack appeared at Zone 8, Mountainhouse Creek, and either the 0.01-in crack or delamination for pipe segments comprising various pipe strengths installed at Cross Canyon (see also Table 1). Assuming that the same construction procedures as those used for an entrenched pipe with ordinary structure backfill are employed, with rigid inspection to assure compliance with construction specifications, the upper plotted line in Figure 24 provides suggested ultimate overfill

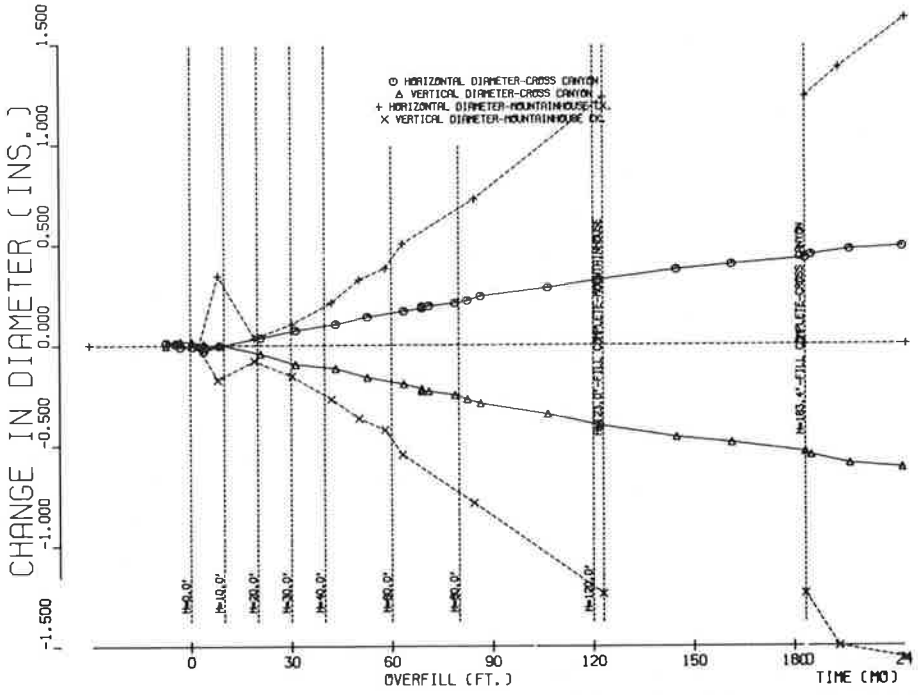

Figure 23. Comparison of diameter changes in Zone 4, Cross Canyon, with those in Zone 8, Mountainhouse Creek.

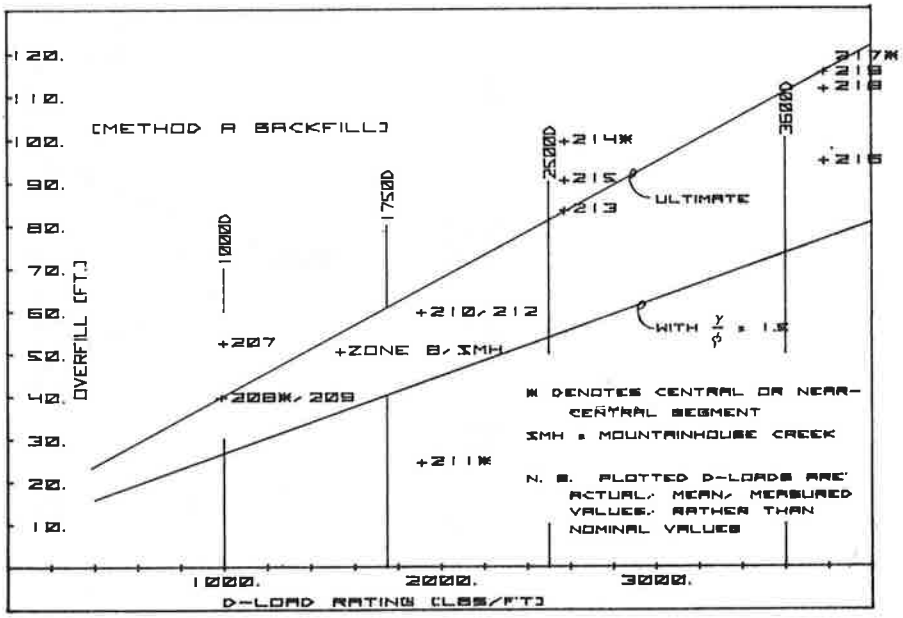

Figure 24. Plot of ultimate and recommended maximum overfills for various pipe strengths based on first appearance of 0.01-in crack or delamination.

limits for pipes of various strengths. A second line based on a safety factor (γ/ϕ) of 1.5 depicts recommended design overfills.

Zone 5 (1750D Pipe)

Much evidence favors the opinion that the central segment (211) in Zone 5 behaved in an anomalous manner. Toward the end of the project, it was learned quite by accident that the pipe manufacturer had used smooth, undeformed inner bars in Zone 5 only, which explains at least a portion of this zone's anomalous behavior for reasons to be noted later in this paper.

Although there was, in general, satisfactory agreement between quasi-theoretical and experimental parameters (e.g., bending moments and displacements), behavior of the central segment was quite different from that of two adjoining segments in this zone and also from that behavior which might have been expected from consideration of segments in other zones.

Central Segment 211 exhibited the 0.01-in crack at a lower overfill (24 ft) than did any of the other segments in any zone. Adjoining Segments 210 and 212, also in Zone 5, did not exhibit the 0.01-in crack until the overfill reached 60 ft.

Segments in this zone exhibited significant delamination above 80 ft of overfill--experimentally measured displacements typically begin to exceed

Table 1. Date and overfill at time of failure.

		Point of Failure[a]					Point of Failure[a]		
			Overfill					Overfill	
Zone	Segment	Date	Meters	Feet	Zone	Segment	Date	Meters	Feet
1	202	01/02/75	18.9	62.0	7	216	04/23/75	28.8	94.6 (delamination)
	201	01/09/75	20.6	67.4		217	05/02/75	35.1	115.2 (delamination)
2	202	12/10/74	15.4	50.6		218	05/01/75	33.9	111.3 (delamination)
	203	12/23/74	17.3	56.7		219	05/02/75	35.1	115.2 (delamination)
3	204	12/10/74	15.0	49.1	8	220	-	-	-
	205	01/02/75	18.7	61.2		221	-	-	-
	206	12/31/74	18.2	59.6		222	01/03/75	18.6	61.0
4	207	12/11/74	16.0	52.5		223	-	-	-
	208	12/05/74	12.1	39.6		224	01/03/75	18.6	61.0
	209	12/05/74	12.1	39.6	9	225			
5	210	01/02/75	18.2	59.6		226			
	211	11/21/74	7.4	24.4		227	DID NOT FAIL		
	212	01/02/75	18.2	59.6		228			
6	213	04/18/75	25.4	83.3 (delamination)		229			
	214	04/23/75	30.3	99.3 (delamination)	10	230	01/03/75	17.8	58.4
	215	04/21/75	27.5	90.3 (delamination)		231	12/03/74	11.4	37.4
						232	12/03/74	11.4	37.4
						233	12/10/74	12.9	42.3
						234	01/03/75	17.8	58.4

[a]Actually, first observation of 0.01-in crack or delamination.

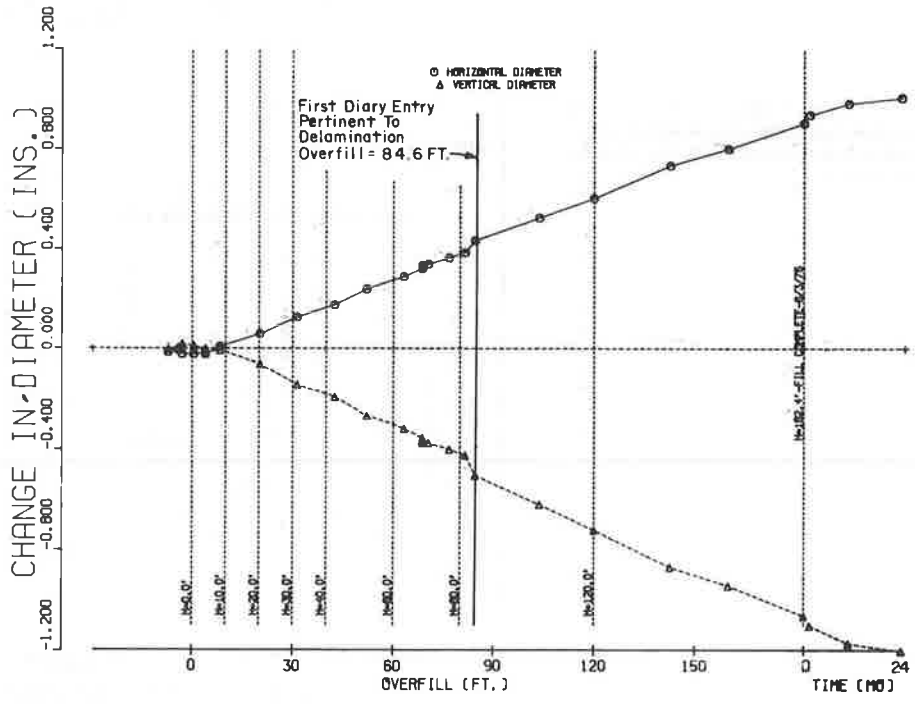

Figure 25. Changes in horizontal and vertical pipe diameters as function of overfill and time after embankment completion, Zone 5.

quasi-theoretical after delamination occurs and the pipe ceases to behave as a usable structure. Overfills at delamination are more accurately identifiable as discontinuities in slopes of the diameter-change curves (Figures 25, 26, and 27).

Diameter changes in the central segment were twice as large as those in Zone 4 (cf. Figures 23 and 25).

Zone 6 (2500D Pipe)

The 0.01-in crack appeared in Zone 6 for the first time in Segment 215 with an overfill of 99 ft. Delamination was observed at lower overfills: 83 ft in Segment 213; 99 ft in Segment 214; and 90 ft in Segment 215. These criteria have been used in the plot of overfills for acceptable behavior (Figure 24).

At any given overfill, effective densities acting on Zone 6 were significantly higher, in general, than those acting on Zones 4 and 5 (cf. Figures 16, 17, and 18).

Up to the 100-ft overfill, diameter changes were 33 percent greater than those in Zone 4 (cf. Figures

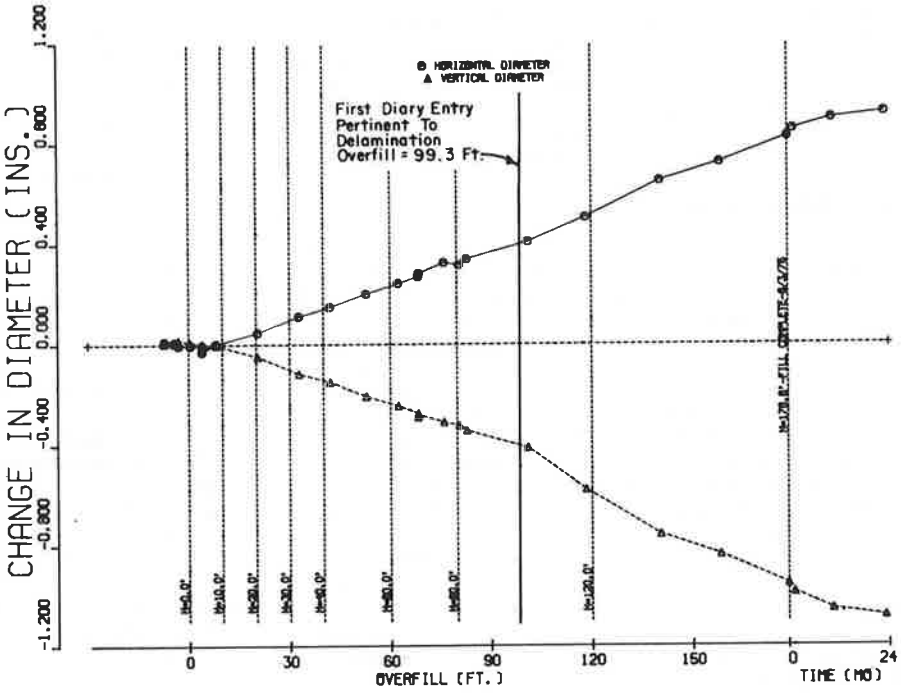

Fgiure 26. Changes in horizontal and vertical pipe diameters as function of overfill and time after embankment completion, Zone 6.

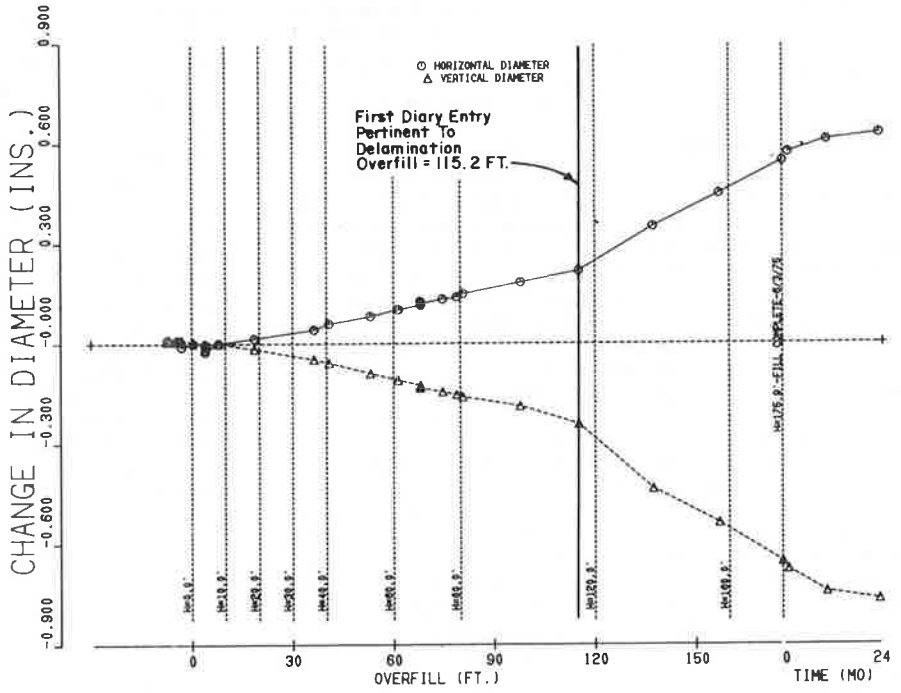

Figure 27. Changes in horizontal and vertical pipe diameters as function of overfill and time after embankment completion, Zone 7.

23 and 26). Above 100 ft, they were twice as great at Zone 6 as those at Zone 4. The Zone 6 pipe, being appreciably stiffer than that in Zones 4 and 5, drew greater load to itself than did the more flexible pipes.

Zone 7 (3600D Pipe)

The 0.01-in crack appeared for the first time in this zone with an overfill of 111 ft in Segment 216 and at an overfill of 115 ft in representative Segment 217 and in Segment 219. Segment 217 also began to delaminate under this overfill. Segment 216 began to delaminate at an overfill of 95 ft but is less representative because it adjoins the more flexible Zone 6.

Diameter changes in Segment 217 were about two-thirds as large as those in Zone 4 up to the 115-ft overfill (cf. Figures 23 and 27), at which point these functions exhibit significant discontinuities at the same time delamination was first observed in the zone. At fill completion, the Zone 7 diametral changes were 25 percent greater than those in Zone 4.

General Observations

A study of distress as manifested by total length of cracking in representative segments is of interest. At the lower overfills, the strongest pipe (Zone 7) exhibited, in general, the least cracking length and Zone 5, the greatest. The most flexible pipe (Zone 4) remained close to the middle-runner position among all zones throughout the entire course of fill construction. Conditions in the stiffer pipes deteriorated more rapidly, and two years after fill completion, based on total crack length, these zones were ranked in the following order: 4, 5, 6, and 7; the most flexible pipe cracked least and the stiffest pipe, the most.

The following are results of observations of three zones (8, 9, and 10) with low-modulus inclusions.

Zone 8 (1000D Pipe with Step-Tapered Polystyrene Plank Inclusion)

Uniaxial laboratory compression tests of small samples of the polystyrene plank demonstrated physical properties conducive to forming good low-modulus inclusions. In laterally confined and unconfined states, specimens were compressed for extended periods of time at varying levels of stress from 1.7 to 21 psi. At the latter level, the material suddenly collapsed.

In the field installation, normal soil stresses acting on the pipe increased gradually under the polystyrene until some point was reached between the 80- and 120-ft overfills when stresses were approximately 21 psi, after which there was no increase.

It is hypothesized that by the time the limiting stress capacity of the polystyrene had been reached, surrounding soil had become sufficiently compact to produce a soil arch so that the soil would not move into the collapsing polystyrene. As a result, this zone ultimately exhibited the most uniform distribution of low effective densities around the upper 240° of pipe periphery of all zones.

Two factors produced some cracking, however: (a) a large concentration of soil stress at the invert, which was characteristic of all zones, and (b) a large diminution of compressive thrust at the crown due to reduction of lateral soil stress by the polystyrene at the sides of the pipe (Figure 28). The tensile stresses at the crown due to heavy invert gradients in soil stresses could not be sufficiently reduced by the small compressive thrust stresses, and cracking occurred.

Diametral changes at Zone 8 were two-thirds as large as those in Zone 4 but seven times as great as those in Zone 9 (cf. Figures 23, 29, and 30); these differences must be attributed to relative lack of lateral support.

Zone 9 (1000D Pipe with Uncompacted Soil in Trench Surmounting Culvert)

The performance of Zone 9 proved superior to that of any other zone. While the observed distribution of soil stress appeared much less uniform, hence less favorable than that in Zone 8 (cf. Figures 19 and 20), the existence of more lateral support than in Zone 8 resulted in greater crown thrusts and hence less cracking (cf. Figures 23, 31, and 32).

Two years after fill completion, the maximum crack width in central Segment 227 was only 0.005 in, so the representative segment in this zone, unlike any other, never exhibited the 0.01-in crack.

Correlations between quasi-theoretical and observed cracking limits were satisfactory, although observed cracking limits were broader than quasi-theoretical. This phenomenon was very typical, which suggests that the 400-psi theoretical cracking stress chosen was too high.

Maximum diameter change was 0.05 in, much smaller than those in Zones 1 through 8 and about half that in Zone 10 (cf. Figures 30 and 33, noting difference in vertical scales).

Zone 10 (Baled-Straw Layer Surmounting Pipe)

Effective-density distributions (see Figure 21) in this zone exhibited sharp gradients in the upper and lower halves of the pipe. Such gradients were typical at the invert in all zones because of a large concentration of soil stress at the invert-bedding interface. At the crown, greatly reduced soil stresses under the straw combined with large stresses in the upper quadrants to produce large stress gradients that tended to dampen with increasing overfills.

Large bending moments in the pipe walls were the natural result of these stress gradients and produced significant early cracking. The 0.01-in crack was first observed under a relatively low overfill of 37 ft (see Table 1).

Above 60 ft of overfill, density gradients in the upper half of the pipe became small; a crown density 8 percent of embankment density transitioned smoothly to 0.3w at the springing line (see Figure 21).

Based on considerations of total crack length, and to some extent other factors, beneficial effects of low-modulus inclusions were more in evidence for deeper overfills. For overfills from 0 to 25 ft, Zones 6 and 7 (the 2500D and 3600D pipes) behaved better than Zone 9 (1000D with uncompacted soil); Zone 4 (the 1000D pipe) was better than Zones 8 and 10 (1000D with polystyrene plank and baled straw, respectively).

At 26 ft, Zone 9 had surpassed all zones but the very stiff Zone 7, but Zones 4 and 6 were still ahead of Zones 8 and 10.

At 66 ft, Zone 9 had surpassed Zone 7, and Zone 8 was below Zone 7 but better than Zones 4 and 6, which were still better than Zone 10.

From 130 ft to fill completion and 24 months beyond, Zones 9, 8, and 10, in that order, were in the best condition and crackwise were in about the same condition. Meanwhile, next in quality of behavior were Zones 4, 5, 6, and 7, in that order, which suggests the interesting anomaly that the degree of cracking distress was better for the more flexible pipes.

Based on considerations of diameter changes and cracking at Cross Canyon, Zone 9 was clearly better than any of the other zones. None of the low-modulus inclusion zones exhibited delamination.

Despite what might have been deemed inferior behavior of Zones 8 and 10 at the lower overfills, they demonstrated relatively small changes in distress beyond the 70-ft overfill, which suggests a potential for use of even higher fills with these construction methods. From 70 to 159 ft, a 127 percent increase in overfill, the total crack length in Zone 8 changed by only 5.5 ft (from 91.1 to 96.6 ft), or 6 percent; that in Zone 9, by 1.9 ft (from 93.1 to 95.0 ft), or 2 percent; and Zone 10, by 4.4 ft (from 92.6 to 97.0 ft), or 5 percent.

Comparison of behavior of Zones 8, 9, and 10 emphasizes the necessity for considering more than one factor in distress development. Large soil-stress gradients in Zone 9 should have been conducive to large bending moments and hence a high incidence of cracking. However, large lateral soil stresses produced large compressive crown thrusts, which reduced the tensile stresses and hence the cracking at the inner periphery of the pipe.

Figure 28. Quasi-theoretical thrusts, Zone 8.

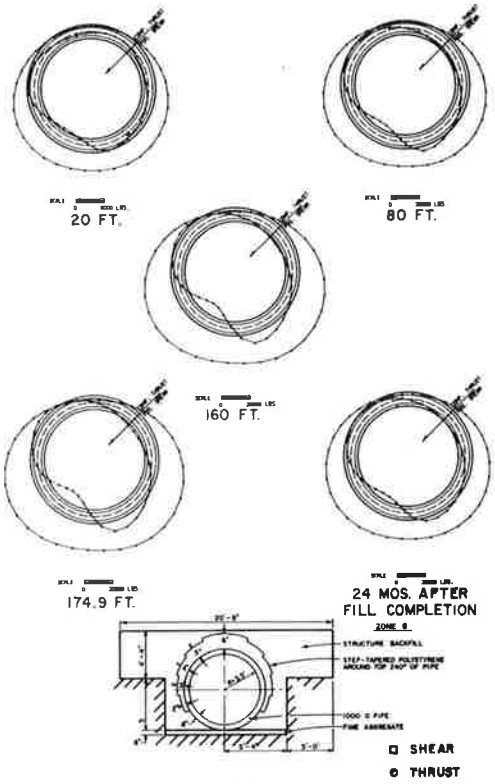

ANALYSIS OF PRESTRESSED PIPE

In order to establish a background of quasi-theoretical parameters for the functional prestressed pipe under 200 ft of earth fill for comparison with measured ones, a second neutral-point analysis was developed, patterned after theory found in Ameron's Prestressed Concrete Cylinder Pipe (28) with some modifications.

The researchers anticipated more difficulty interpreting measured internal strain data from the prestressed pipe walls than in the case of the reinforced-concrete pipe for several reasons: (a) early placement of pipe segments after casting superimposing creep and shrinkage strains due to prestressing on those due to earth loads and (b) the large ratio of wall thickness to pipe radius (approximately 1:2), which produced a nonlinear (hyperbolic) strain diagram.

Anticipating the first problem, the researchers placed a control segment of similar prestressed pipe in a comparable but essentially unstressed environment. The Zone-12 (control) segment was placed on end near the toe of the embankment and covered (outside only) to the level of its upper end. Thus, the segment was not completely unstressed; however,

Figure 29. Changes in horizontal and vertical pipe diameters as function of overfill and time after embankment completion, Zone 8.

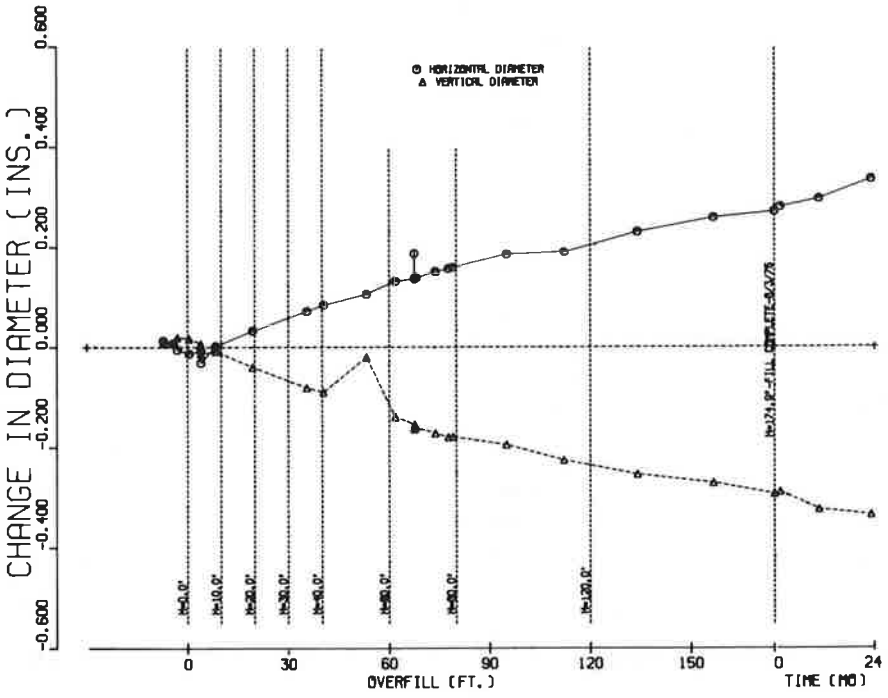

stresses due to the surrounding soil were very small compared with those due to the 200-ft overfill at Zone 11. More variations in ambient air temperature within the control segment might be expected than in Zone 11.

The Zone-12 strains were plotted as functions of time with a datum at June 18, 1974, the date of casting the Zone-12 segment (see Figures 34 and 35); the Zone-11 segment was cast on June 27, 1974. Most of this strain may be seen to have occurred during the first 110-120 days and may be attributed to normal creep and shrinkage.

Subsequent to this initial period, there was a prolonged, general gradual trend toward higher com-

Figure 30. Changes in horizontal and vertical pipe diameters as function of overfill and time after embankment completion, Zone 9.

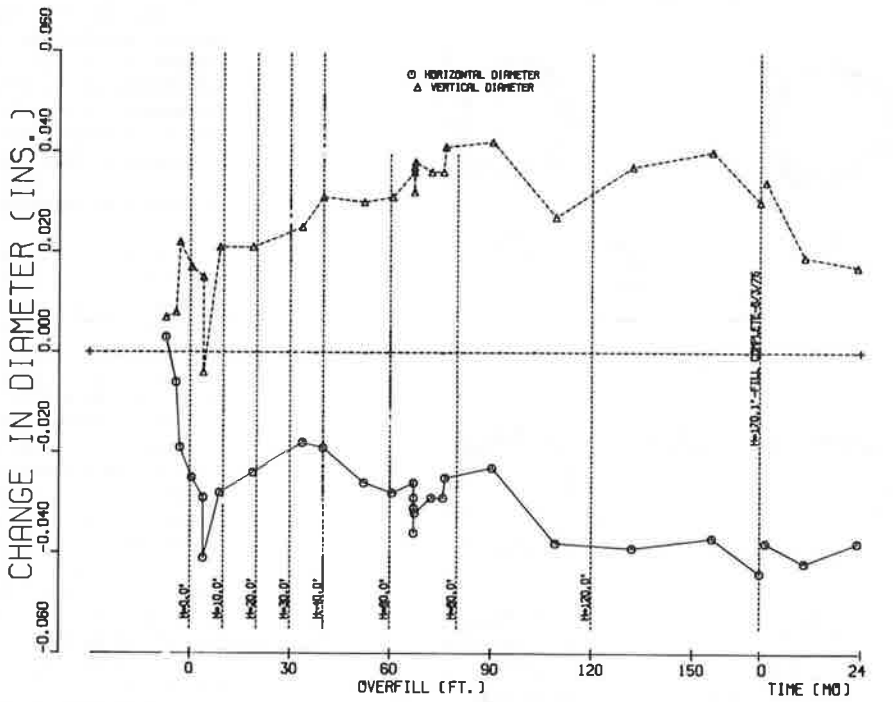

Figure 31. Quasi-theoretical thrusts, Zone 9.

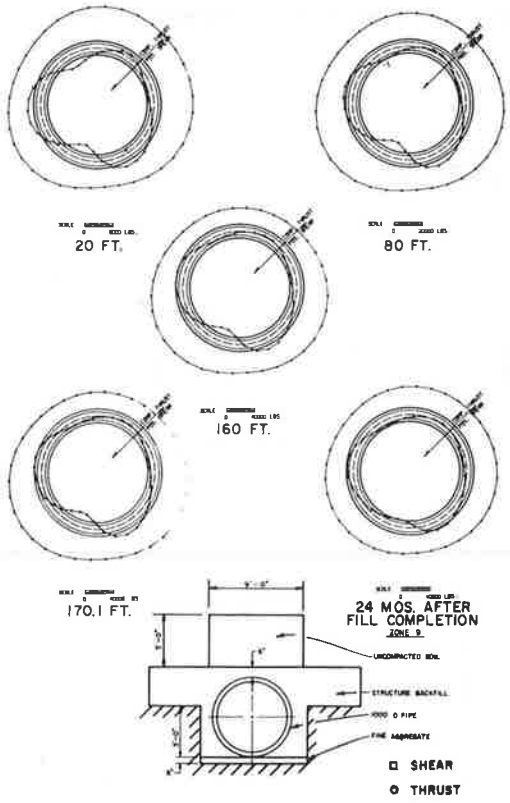

Figure 32. Quasi-theoretical thrusts, Zone 10.

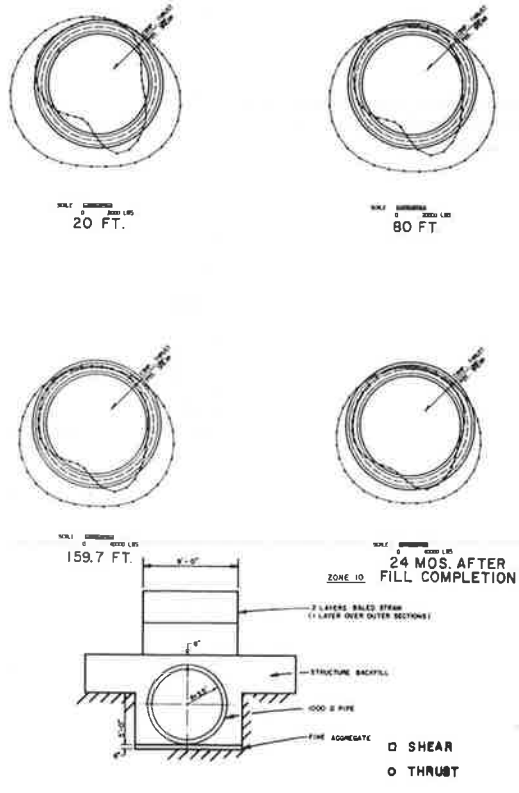

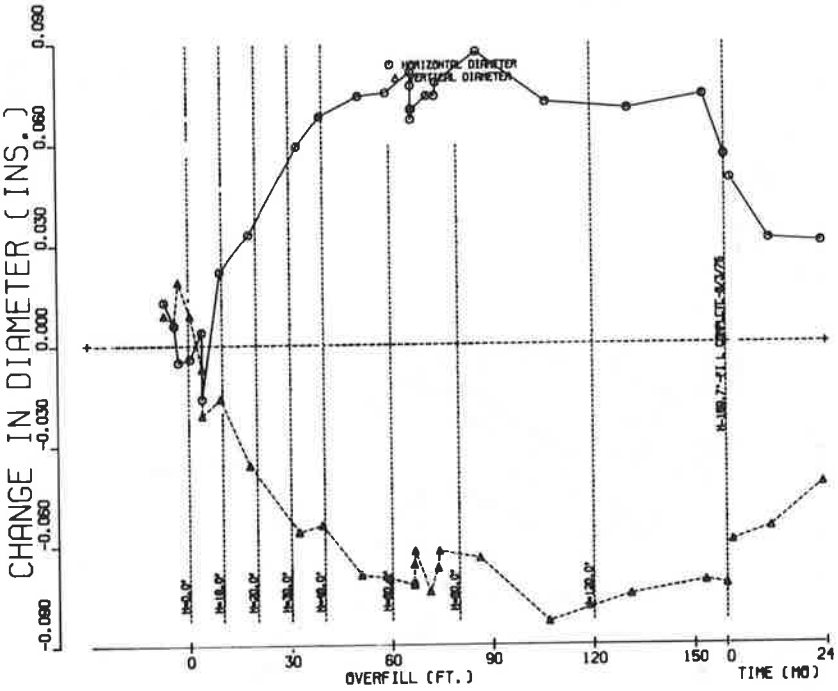

Figure 33. Changes in horizontal and vertical pipe diameters as function of overfill and time after embankment completion, Zone 10.

pressive strains with superimposed trends of shorter duration in a reversed, tensile direction. Such a trend is clearly visible between Days 110± and 350±, during which period the embankment was being constructed. Since this period encompassed the fall, winter, and spring seasons of 1974-1975, tensile trends may logically be attributed to absorption of moisture from the humid atmosphere or from embankment material.

There exists a very large amount of scatter in the readings from the Carlson strain meters embedded in the brush coats; they vary from roughly 130 to 320 microin/in (see Figure 34). The strain pattern shows a possibly significant localization; larger strains are in positions 1, 2, 7, and 8 on the top half of the segment, and smaller strains are in positions 3, 4, 5, and 6 on the bottom half. This phenomenon might have resulted from an increased loss of moisture due to insolation and consequent increased shrinkage during the postcuring storage period prior to pipe placement in the embankment; the top half of the pipe was placed on the sunny side and the bottom half in shadow. This large variation in strain by itself would have virtually precluded use of control Segment 12 for adjustment of Zone-11 strains.

The observed variation in strains in the midplane Carlson meters was much smaller (see Figure 35). Buried almost a foot from either pipe surface, this portion of the concrete was less susceptible to moisture variations and exhibited a strain range of 32-38 microin/in. The researchers elected to consider these Zone-12 midplane strains representative creep and shrinkage strains over the entire depth of the pipe wall. Only the computed thrust is affected.

A typical cross section of unadjusted strains measured at Zone 11 during embankment construction is given in Figure 36, which shows an incompatible strain pattern characteristic of all plots. Straight regression lines could not be fitted to strain readings. Parabolic regression curves could be plotted that closely approximated all strains except those in the brush coats, which were almost invariably on compressive sides of the parabolas. This phenomenon has a logical explanation. The rich gunite mixture air-blown around the surface of the hardened core should exhibit large shrinkage. As brush coats shrink against the restraint of the already shrunken core, extensive longitudinal cracking must develop. The relatively long Carlson minimeters may span a number of such cracks, and when cracks close under embankment loads, strain meters produce readings that are unrepresentative on the compressive side and incompatible with strain patterns in the core. The researchers elected to ignore brush-coat strains and approximate patterns of core strains by regression parabolas.

A new zero strain datum was plotted and coordinates were transformed to produce equal compressive and tensile areas between the parabolas and the new base lines. Thrust factors (T/E_C) were subsequently computed as products of the area of the transformed pipe cross section and differences in strains between old and new base lines; bending-moment factors (M/E_C) were computed as integrated products of the stress areas and lever arms about new x_0-axes.

The values of M/E_C and T/E_C were subsequently modified by a factor, E_C (= 3000 ksi), to produce experimental values of bending moments and thrusts in the pipe wall due to overburden for a number of significant overfills. Experimental values are compared with quasi-theoretical values of the same parameters from the neutral-point program and measured soil stresses for maximum overfill in Figures 37 and 38. Quasi-theoretical wall displacements are compared with extensometer measurements in Figure 39. The commensurate, observed distribution of effective densities about the pipe periphery, based only on Cambridge contact stress-meter readings, is plotted in Figure 40. Correlations between quasi-theoretical and measured parameters were extremely good.

ANALYSIS OF SETTLEMENTS

A method of analysis whereby earth loads acting on the crown of a buried conduit could be predicted

Figure 34. Zone 12, plane-1 (brush-coat) strains.

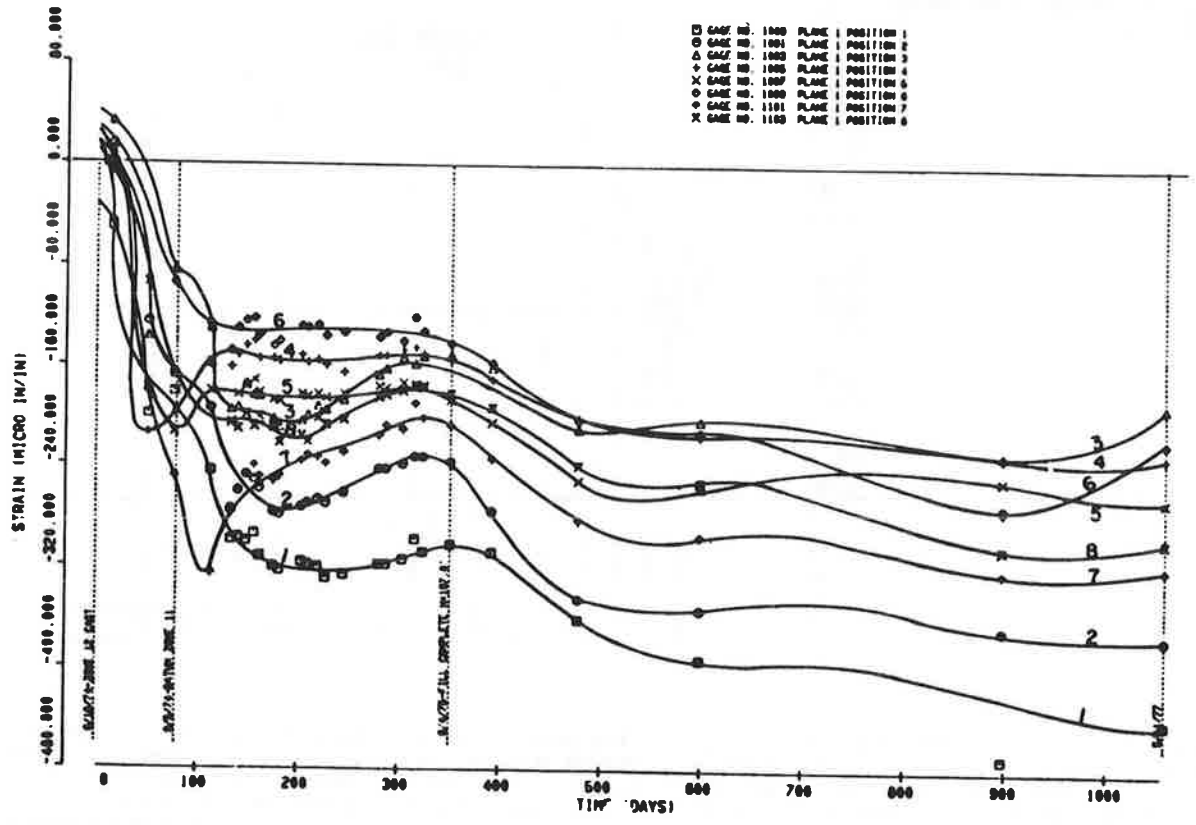

Figure 35. Zone 12, plane-2 (midplane) strains.

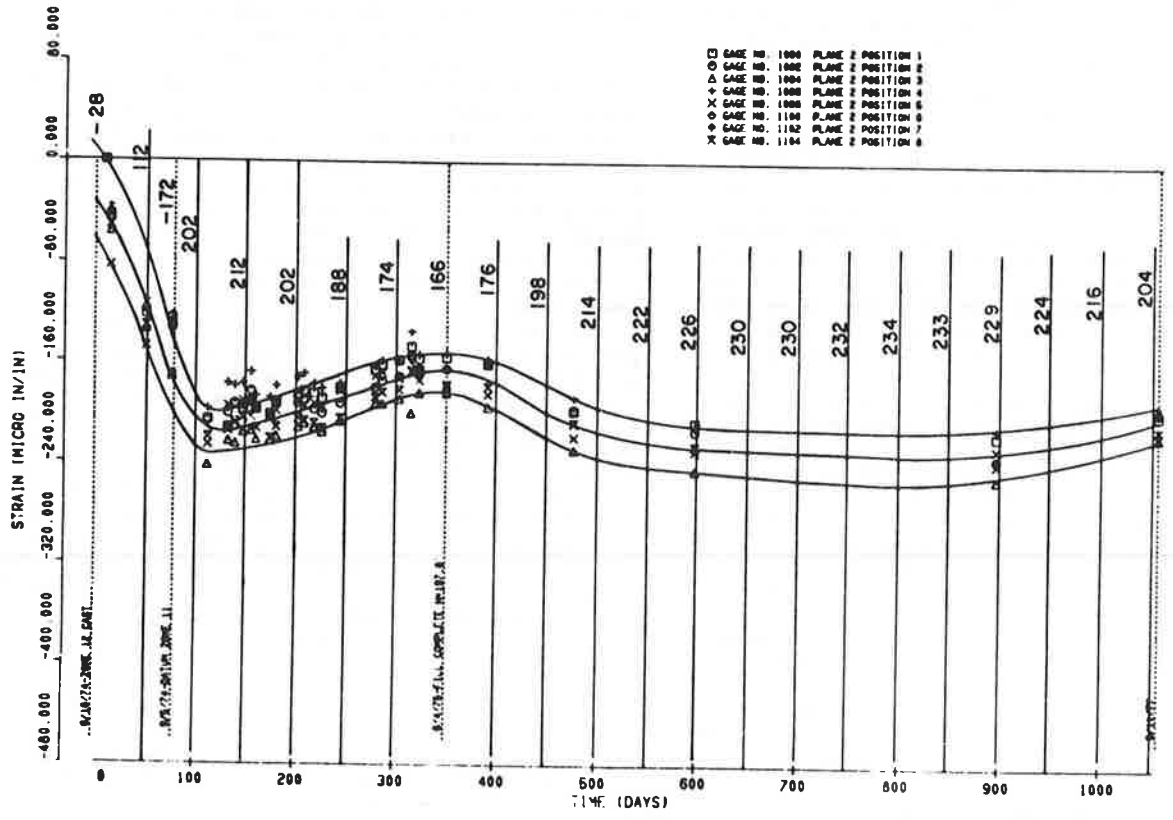

Figure 36. Typical strain cross section for prototype (Zone 11).

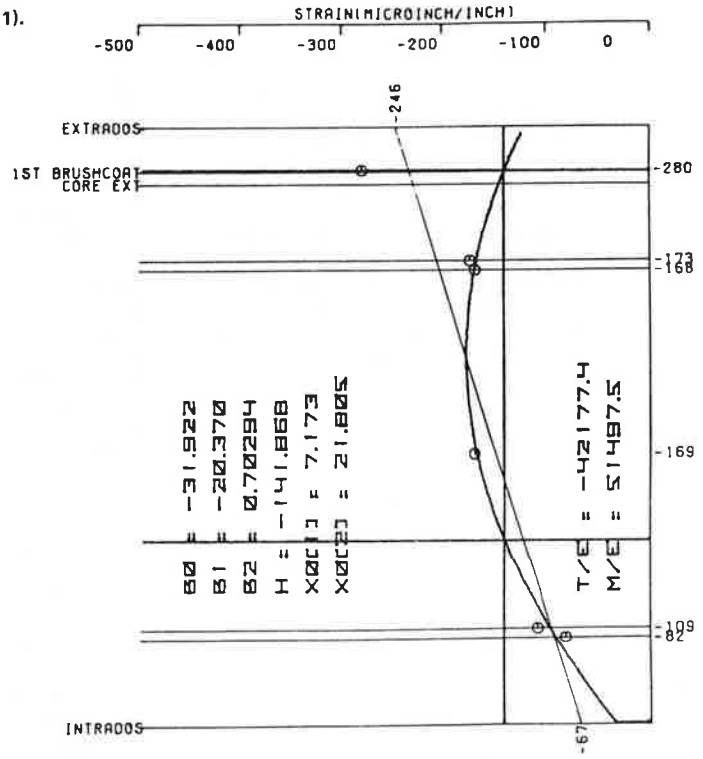

Figure 37. Quasi-theoretical versus experimental bending moments, maximum overfill.

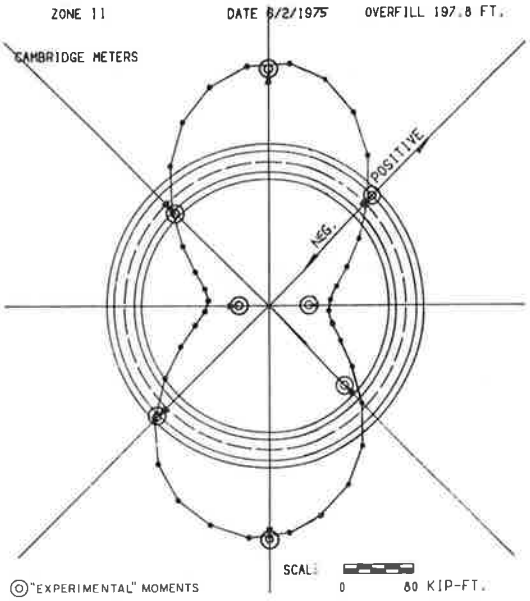

Figure 38. Quasi-theoretical versus experimental thrusts, maximum overfill.

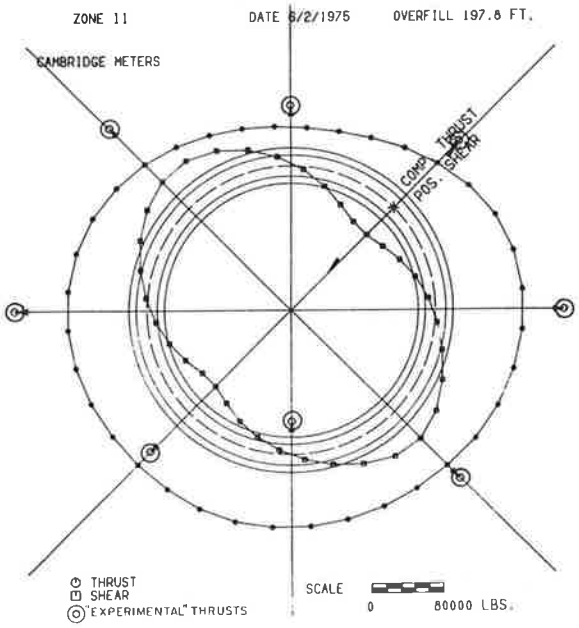

from assessment of differential settlements between the conduit centerline and the exterior prisms was developed by Marston, Spangler, Costes, and others (24, Section 6). For several decades this method, commonly described as settlement-ratio analysis, has been employed by engineers as a mainstay among design procedures for buried pipes.

At Cross Canyon, sophisticated measuring equipment produced a significant body of differential-settlement data for the embankment and pipe and strains in low-modulus inclusions. Comprehensive analyses of data have been made to compare experimentally measured crown loads with quasi-theoretical loads obtained from settlement ratios. Two solutions were examined in which (a) settlement ratios were determined from field measurements at Cross Canyon and (b) ratios recommended by Spangler on the basis of statistical studies of numerous field installations were used.

Figure 41, which is typical, provides comparisons

of calculated crown loads for various values of $r_{sd\rho}$ recommended by Spangler and for various quasi-theoretical values of $r_{sd\rho}$ based on field measurements; soil stresses are measured by stress meters at the crown and in the embankment above the crown for Zone 1. The plotted quasi-theoretical and recommended crown loads are, by comparison with measured ones, very high. Poor correlations were typical of all zones but Zone 9.

For induced-trench Zones 9 and 10, settlement ratios calculated from field data closely approximated the range of -0.3 to -0.5 recommended by Spangler. Encouraging correlations were obtained at Zone 9 between quasi-theoretical and measured crown loads by using Costes' approach, but Spangler's methods still produced very high crown loads compared with measured ones. For Zone 10, neither Spangler's nor Costes' approach produced valid results. Spangler's recommended values of r_{sd} failed to predict nonlinearity of observed functions of soil stress and overfill, especially for Method-B (low-modulus inclusion) installations.

In 1955, Costes modified Spangler's assumptions and presented a method by which an induced-trench culvert may be analyzed by using the same force diagram that Spangler used but taking into consideration differences in moduli of compaction of embankment and trench materials and the broad range of possibilities for the parameter $K\mu$. Implementation of Costes' method of analysis would be difficult unless extensive testing of fill and trench material were performed prior to design of a culvert. Closer predictions of crown stresses could be made if such testing could be performed economically. A less exact but more practical approach is to use average values for physical properties based on statistical analyses of similar materials; however, as was noted in analyses of Zones 9 and 10, this method is still not completely reliable.

Based on Cross Canyon studies, the settlement-ratio method of analysis is not reliable for predicting crown loads, and, especially for rigid conduits or deep embankments, the information it provides is not sufficient to make reasonable assessments of supporting strengths of culvert-soil systems.

Figure 39. Quasi-theoretical versus experimental wall displacements, maximum overfill.

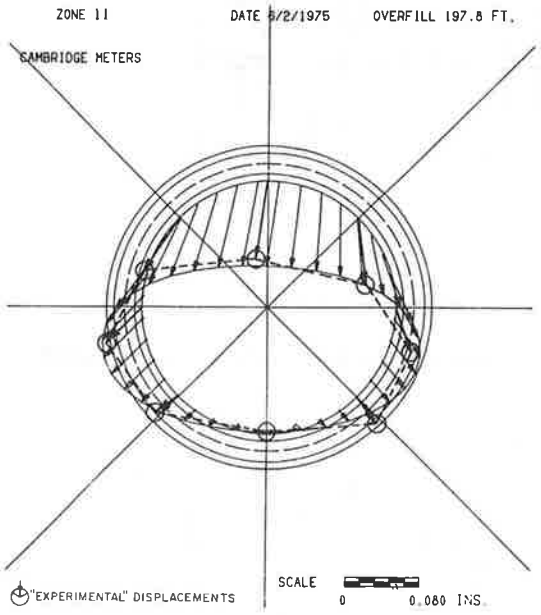

Figure 40. Observed effective-density profile, Zone 11, maximum overfill.

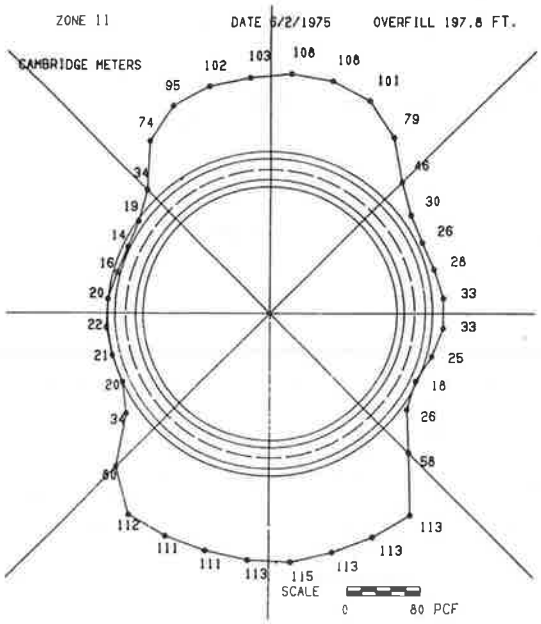

ANALYSIS OF COSTS

Costs per unit length of each test zone were calculated from bid prices to provide comparisons of relative economy of construction methods. Because of

Figure 41. Comparisons of measured soil stresses and those from settlement-ratio analysis, Zone 1.

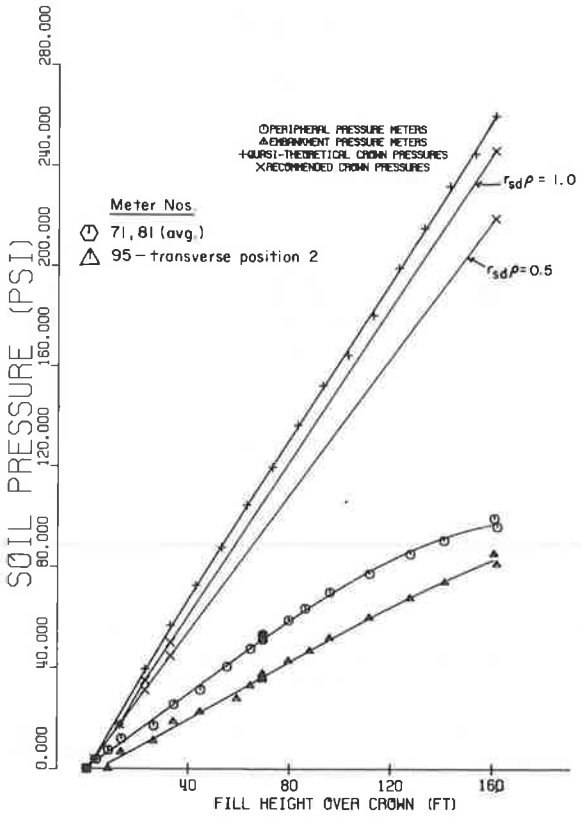

the highly specialized nature of the work, short zones, delays caused by instrumentation, etc., costs should be considered in a relative, not absolute, sense:

Zone	Cost ($) Per Linear Foot	Per Meter
2	152.08	498.81
4	163.42	536.02
1	164.88	540.79
3	168.29	551.99
9	171.75	563.35
5	173.42	586.82
8	184.44	604.95
6	188.42	618.02
10	193.01	633.07
7	209.28	686.43
11	493.16	1617.56

CORRELATIONS OF CROSS CANYON DATA WITH HEGER'S CRITERIA

Heger has published design equations for reinforced-concrete pipe distress as background criteria for a proposed design method. Four modes of distress are considered: crack control (appearance of the 0.01-in crack), radial tension, diagonal tension, and ultimate flexure. These criteria were developed from statistical analyses of data from a large number of three-edge bearing tests.

The 0.01-in crack is a particularly convenient criterion, primarily because it has traditionally been used as a significant point in the three-edge bearing test in the United States and Europe. This crack width is considered by many culvert designers as the limit beyond which corrosion of reinforcing steel poses a significant threat.

Delamination, or bowstringing, due to excessive radial tension is considered by the researchers to be a more important form of distress than cracking for several reasons:

1. Surface cracking is readily visible and may be repaired by patching with the expectation that structural integrity will not be significantly impaired.
2. Delamination may be observed only at the ends of pipe segments at open joints.
3. When delamination occurs, the inner or outer shells of the pipe wall and reinforcing cages cease to function structurally and the pipe loses a portion of its supporting capacity; this weakening is apparent from visible discontinuities in functions of diameter change and overfill and in deteriorations in correlations of quasi-theoretical and observed wall displacements.
4. Repairing delamination is difficult and offers little hope of restoring structural integrity.

Shear failure in pipe walls is more critical than delamination. The typical crack crosses the entire wall, and there may be radial wall displacement on one side of the crack relative to that on the other and resultant exposure of reinforcing cages.

Ultimate flexure may be observed in two phases, which involve yielding of the inner reinforcing bars at invert and crown and subsequent yielding of the outer bars at the springing lines to form four plastic hinges and possibly to induce pipe collapse.

Heger's equations may be used to predict these failure modes. We investigated their validity in the Cross Canyon installation.

The 0.01-in crack and delamination have been commonly observed during Caltrans pipe research, at least one shear failure has been observed, and ultimate flexure has also occurred. These distress modes do not occur in all instances in the same chronological sequence, and some modes may occur exclusively of others. At Cross Canyon, Zone 3, the first 0.01-in crack was observed at 61 ft of overfill, delamination at 175 ft. At Zone 5, the first 0.01-in crack was observed at 24 ft of overfill, delamination at 85 ft. Delamination and the 0.01-in crack were first observed at Zone 6 at about the same overfill (99 ft). Zones 4, 8, and 10 all exhibited the 0.01-in crack without delamination, whereas Zone 9 experienced neither failure mode.

At Mountainhouse Creek, Part 1, entrenched Zones 7 and 8 cracked, but for the almost fully positive-projecting Zone 9, the dominant mode of distress was pronounced "bowstringing." Zone 10, supported on any unyielding, 60° concrete bedding, failed in shear at one edge of the bedding, and one side of the wall moved inward 16 in relative to the other side. A shearing failure also occurred at Zone 11 as the pipe settled into a soft polystyrene bedding and encountered passive resistance from the soil outside the bedding. Positive-projecting Zones 9 through 12 at Mountainhouse Creek, Part 1, exhibited ultimate flexure by cracking of the invert and crown and crushing of the concrete at the springing lines. Cores taken from the entrenched 4000D Mountainhouse Creek, Part 2, exhibited incipient delamination but no surface cracking.

The equations furnished by Heger demonstrate that appearance of various failure modes depends on differing combinations of bending moment, thrust, and shear, which explains the aforementioned phenomena. For these reasons, much caution must be exercised in establishment of specified effective-density profiles for use in design. A profile that is not representative for a given construction condition may indicate stresses that are conservative for one failure mode and neglect to predict another mode.

In the establishment of such specifications, certain premises should be considered that seem sufficiently self-evident to be axiomatic; still, the researchers encountered sufficient inertia in their acceptance by other engineers to make them worth open discussion. The debatable premises are as follows:

1. In the general case of culverts embedded in deep embankments, the functions for soil stress and overfill will be nonlinear, although they may, under certain unique circumstances, be linear for embankments with or without low-modulus inclusions.
2. Typical effective-density profiles observed by Caltrans researchers for culvert installations with and without soft inclusions have been characterized by density minima at the crown and centers of lower quadrants (12:00, 4:30, and 7:30 o'clock) and density maxima at the invert and centers of the upper quadrants (1:30, 6:00, and 10:30 o'clock). Density gradients are more severe at low overfills but dampen toward more uniform distributions at higher overfills.
3. Because of items 1 and 2 above, it is unsafe to consider only the effective-density profile observed at time of fill completion to establish specifications. The embedded pipe culvert is statically indeterminate and must be checked at all construction levels for design safety.
4. A specified effective-density profile that envelopes all observed profiles for a given culvert does not necessarily produce a more conservative design than the encompassed profiles. The fact that observed density profiles fall essentially within certain bands of loading does not prove these latter to be safe for design specifications.
5. Because moments, thrusts, and shears in differing combinations produce different distress modes

and because of item 4 above, it is essential that specified density profiles be representative in the sense that they are of approximately the same configurations as might be expected for given construction conditions.

6. There is no justifiable reason for designing culverts with soft embankment inclusions for the same profiles as those without inclusions, or for very rigid and very flexible pipes, or for two similar pipes under similar construction modes at very different overfills. Culvert design specifications should differ for differing construction modes and for different ranges of overfill. A design for any given overfill should be checked at upper limits of lower overfill ranges by using appropriate density profiles for those ranges. Designs should be checked for all potential modes of distress at these levels. It is of little significance that a design does not suggest a shear failure under a deep overfill if irreparable delamination is indicated under more severe soil stress gradients characteristic of some lower overfill.

For very expensive culvert installations, where distress is not permissible, a finite-element analysis of the culvert and embankment may be useful. In addition to the expense and delays required by the analysis, the designer must consider the need for site surveys (to establish important boundary conditions); effects of clearing, grubbing, and stripping on such conditions; and the need for developing realistic embankment-material properties through soil classification or triaxial testing of samples from potential sources. If the installation does not warrant this expenditure of effort and money, the designer must use specified density profiles based on observations of past installations and weigh the risks involved in the possibility that construction conditions may produce very different soil-stress distributions.

In addition to making studies of finite-element programs such as REA, CANDE, and NUPIPE, we have advocated certain profiles of effective-density coefficients based largely on observed verified soil-stress distributions at Cross Canyon. The researchers suggest use of these coefficients in conjunction with anticipated embankment densities to establish effective-density profiles, to be converted in turn to soil-stress distributions for input to Caltrans' computerized neutral-point analysis. Output parameters would be evaluated on the basis of Heger's criteria for various possible distress modes.

Studies of Heger's criteria produced the following comparisons:

1. Crack control (f_s.01): Quasi-theoretical inner-reinforcing-bar and concrete stresses output from the neutral-point program were evaluated at overfills at which the 0.01-in crack first appeared, according to the field research coordinator's diary (see Table 2).

Smooth cold-drawn wire was used for inner bars at Zone 5 only. Heger's equations for this type of reinforcement use different coefficients than those for hot-drawn deformed bars, which explains at least part of the anomalous behavior of this zone, and its classification as 1750D is even questionable. It is of interest that calculated stresses exhibit encouraging agreement even when they are greater than the

Table 2. Comparisons of quasi-theoretical stresses at 0.01-in crack with those from Heger's criteria.

Zone	Inner-Reinforcing-Bar Stresses (psi)	
	Maximum Quasi-Theoretical	Heger's Criteria[a]
3	92 000	
4	60 000	
5	37 000	
6	56 000	
8	70 000[b]	
10	69 000	
Avg 1000D[c]	72 750	72 200
Avg 1750D[d]	37 000	36 700
Avg 2500D[e]	56 000	36 000

[a] f'_c = (6000 psi).
[b] See Figure 9.
[c] Zones 3, 4, 8, and 10.
[d] Zone 5.
[e] Zone 6.

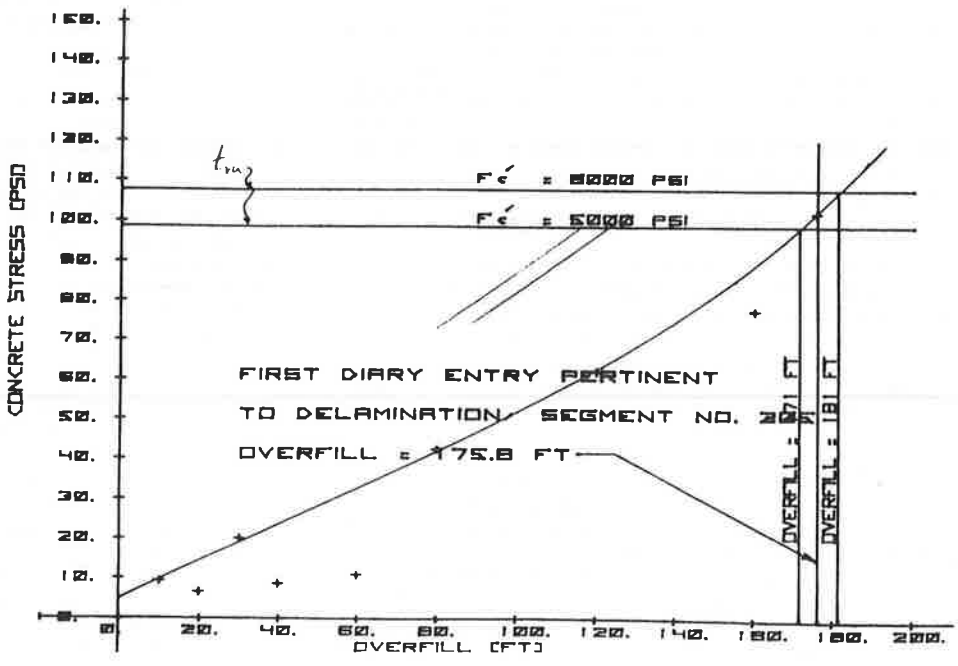

Figure 42. Radial tension stresses computed from Heger's criteria compared with 1.4fc', Zone 3.

f_y (=58 000 psi), which is an upper bound in the criterion.

2. Incipient delamination: Figures 42 and 43 show plots of radial tension stress (t_r) as functions of overfill for Zones 3 and 4 compared with t_{ru} $[=1.4(f_c')^{1/2}]$ for f_c' = 5000 and 6000 psi. Intersections of plots of t_r with t_{ru} should mark overfills at which delamination might be expected to begin. Plots for Zones 8, 9, and 10, for which no delamination was observed, showed curves of t_r not intersecting t_{ru}, whereas similar plots for Zones 5 and 6 closely predicted delamination overfills.

Also included is Figure 44, in which calculated values of t_r at the invert for a 140V:42H loading for various overfills have been compared with t_{ru}. A comparison of predicted overfills at which delamination would occur for this loading demonstrates that predictions would be highly unconservative for Zones 5 and 6, which delaminated at 85 and 99 ft, respectively, but would unjustly penalize the low-modulus inclusion Zones 8, 9, and 10, where no delamination was observed.

3. Diagonal tension and ultimate flexure: Although distress of these types was very evident at Mountainhouse Creek, Part 1, quantitative data that would allow application of Heger's criteria for these modes of failure are lacking. Either type of failure may have occurred at Zones 1, 2, and 4 at Cross Canyon in the late stages of the project, but they are not specifically mentioned in diaries and overfills at failure cannot be accurately specified.

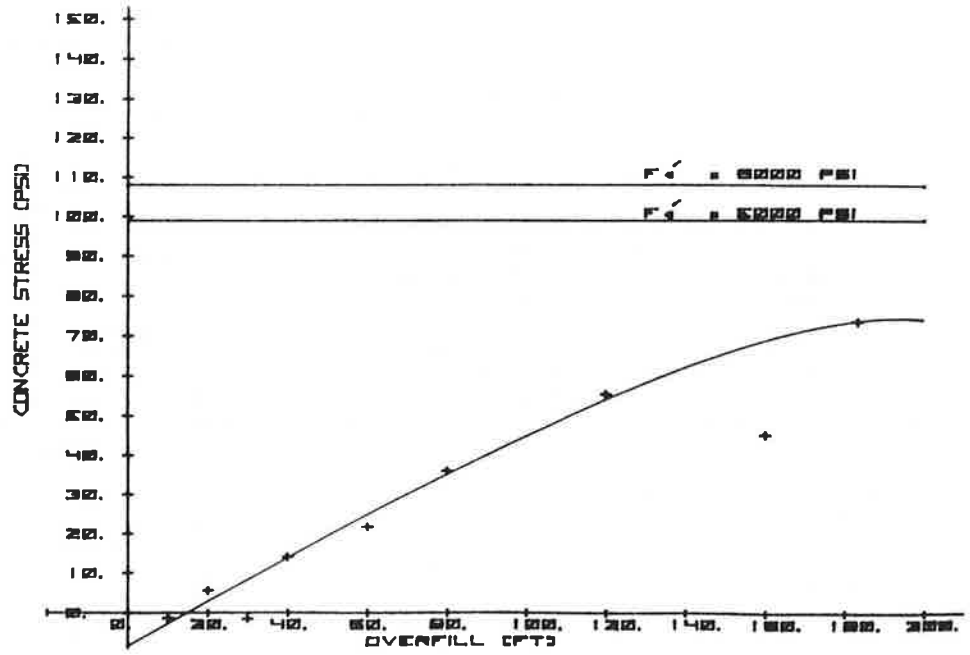

Figure 43. Radial tension stresses computed from Heger's criteria compared with 1.4fc', Zone 4.

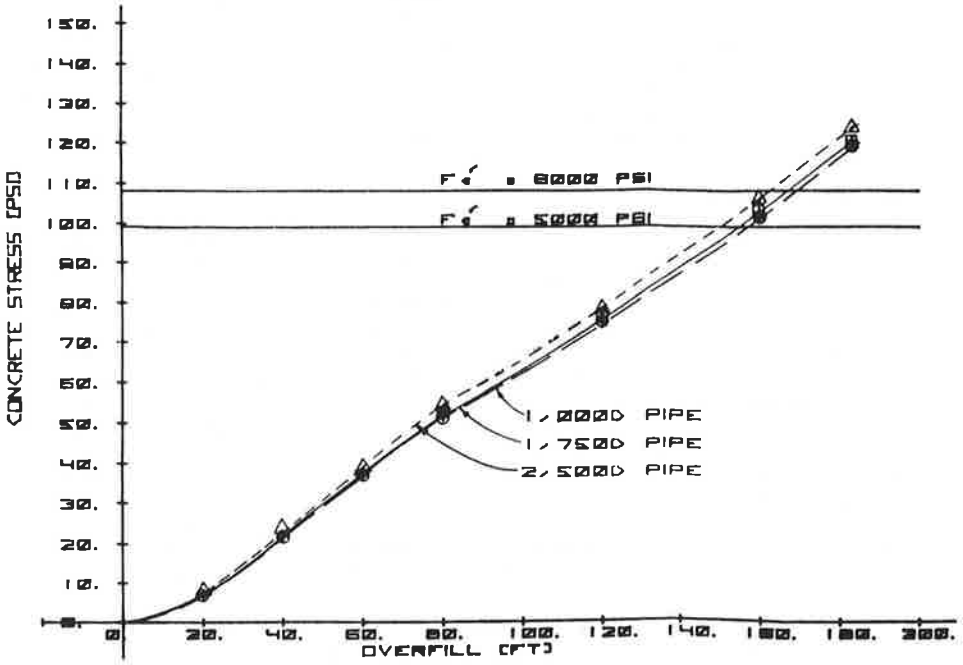

Figure 44. Radial tension stresses computed from Heger's criteria and neutral-point analysis moments and thrusts compared with 1.4fc', 140V:42H soil-stress distribution.

SUMMARY AND CONCLUSIONS

This paper has stressed the importance of using caution in establishment of design specifications for culverts; it should be ascertained that such specifications are representative of those that might occur for given, anticipated construction conditions in order that all possible modes of distress might be accurately evaluated. We caution against use of one or two bands of loading that may envelope all observed profiles and, in some instances, produce similar maximum stresses while failing to predict other, significant modes of failure.

ACKNOWLEDGMENT

Research described in this article was performed in conjunction with a project entitled Rigid Pipe Prooftesting Under Excess Overfills Using Varying Backfill Conditions by Caltrans in cooperation with the Federal Highway Administration, U.S. Department of Transportation.

Opinions, findings, and conclusions expressed in this article are ours and do not necessarily reflect official views or policies of Caltrans or the Federal Highway Administration. This paper does not constitute a standard, specification, or regulation.

REFERENCES

1. R.E. Davis. Structural Behavior of a Reinforced Concrete Arch Culvert. Bridge Department, California Division of Highways, Sacramento, Rept. SSR 9-66, 1966.
2. R.E. Davis and A.E. Bacher. California's Culvert Research Program--Description, Current Status, and Observed Peripheral Pressures. HRB, Highway Research Record 249, 1968, pp. 14-23.
3. R.E. Davis and A.E. Bacher. Forces on Rigid Culverts Under High Fills--Discussion. Journal of the Structural Division of ASCE, Vol. 93, Oct. 1967, p. 105.
4. R.E. Davis and L.R. Patterson. Structural Behavior of a Reinforced Concrete Arch Culvert, Phase 2: Posey Canyon. Bridge Department, California Division of Highways, Sacramento, Rept. SSR 2-68, 1968.
5. R.E. Davis. Structural Behavior of a Flexible Metal Culvert Under a Deep Earth Embankment Using Method B (Baled Straw) Backfill. Bridge Department, California Division of Highways, Sacramento, Rept. R&D 4-69, 1969.
6. R.E. Davis. Structural Behavior of Concrete Arch Culvert. Journal of the Structural Division of ASCE, Vol. 95, No. ST12, Dec. 1969, pp. 2665-2686.
7. R.E. Davis and A.E. Bacher. Structural Behavior of a Reinforced Concrete Arch Culvert, Phase 2: Posey Canyon (Supplemental). Bridge Department, California Division of Highways, Sacramento, Rept. R&D 6-70, 1970.
8. R.E. Davis, A.E. Bacher, and J.C. Obermuller. Structural Behavior of a Concrete Pipe Culvert--Mountainhouse Creek (Part 1). Bridge Department, California Division of Highways, Sacramento, Rept. R&D 4-71, 1971.
9. R.E. Davis. Structural Behavior of Concrete Arch Culvert: Closure and Errata. Journal of the Structural Division of ASCE, Vol. 97, No. ST4, April 1971.
10. R.E. Davis and A.E. Bacher. Concrete Arch Culvert Behavior--Phase 2. Journal of the Structural Division of ASCE, Vol. 98, No. ST11, Nov. 1972.
11. D.W. Spannagel, R.E. Davis, and A.E. Bacher. Structural Behavior of a Flexible Metal Culvert Under a Deep Earth Embankment Using Method A Backfill. Bridge Department, California Division of Highways, Sacramento, Rept. CA-HY-BD-624111-73-6, June 1973.
12. R.E. Davis, A.E. Bacher, and J.C. Obermuller. Concrete Pipe Culvert Behavior (Part 1). Journal of the Structural Division of ASCE, Vol. 100, No. ST3, March 1974, pp. 599-614.
13. R.E. Davis and A.E. Bacher. Concrete Pipe Culvert Behavior (Part 2). Journal of the Structural Division of ASCE, Vol. 100, No. ST 3, March 1974, pp. 615-630.
14. D.W. Spannagel, R.E. Davis, and A.E. Bacher. Effects of Method A and B Backfill on Flexible Culverts Under High Fills. TRB, Transportation Research Record 510, 1974, pp. 41-55.
15. R.E. Davis, A.E. Bacher, and J.C. Obermuller. Concrete Pipe Culvert Behavior (Part 1): Closure. Journal of the Structural Division of ASCE, Vol. 101, No. ST7, July 1975.
16. R.E. Davis and A.E. Bacher. Concrete Pipe Culvert Behavior (Part 2): Closure. Journal of the Structural Division of ASCE, Vol. 101, No. ST7, July 1975.
17. R.E. Davis, A.E. Bacher, and E.E. Evans. Structural Behavior of a Concrete Pipe Culvert--Mountainhouse Creek (Part 2). California Department of Transportation, Sacramento, Rept. CA-DOT-DS-4121-2-75-8, Sept. 1975.
18. R.E. Davis, H.D. Nix, and A.E. Bacher. Structural Behavior of a Reinforced Concrete Arch Culvert--Phase 3, Cedar Creek. California Department of Transportation, Sacramento, Rept. FHWA-CA-ST-4120-01 through FHWA-CA-ST-4120-11, 1977.
19. R.E. Davis and A.E. Bacher. Rigid Culvert Tests--Mountainhouse Creek, Part 1. Concrete Pipe News, American Concrete Pipe Association, Vienna, VA, Aug. 1978.
20. R.E. Davis and A.E. Bacher. Rigid Culvert Tests--Mountainhouse Creek, Part 2. Concrete Pipe News, American Concrete Pipe Association, Vienna, VA, Sept. 1978.
21. R.E. Davis and A.E. Bacher. Behavior of Buried Concrete Pipe: Discussion. Journal of Geotechnical Engineering Division of ASCE, Vol. 105, No. GT3, March 1979.
22. R.E. Davis, H.D. Nix, and A.E. Bacher. Arch Culvert Footing Movements. Journal of Structural Division of ASCE, Vol. 105, April 1979, pp. 729-738.
23. R.E. Davis, H.D. Nix, and A.E. Bacher. Arch Culvert Research--Phase 3. Journal of the Structural Division of ASCE, April 1979, pp. 739-743.
24. R.E. Davis, A.E. Bacher, and others. Rigid Pipe Prooftesting Under Excess Overfills with Varying Backfill Parameters (Sections 1-9). California Department of Transportation, Sacramento, 1978-1982.
25. R.E. Davis, H.D. Nix, and A.E. Bacher. Arch Culvert Footing Movements: Closure. Journal of the Structural Division of ASCE, Vol. 106, No. ST9, Sept. 1980.
26. P.F. Hadala. Effect of Placement Method on the Response of Soil Stress Gages. Proc., Soil Dynamics Conference, Albuquerque, NM, 1967.
27. K.A. Jackura. Instrument for Determining Stress Displacements in Soil. California Department of Transportation, Sacramento, Rept. FHWA/CA/TL-81/09, 1981.
28. Prestressed Concrete Cylinder Pipe. Ameron, Inc., Monterey Park, CA, July 1975.

Publication of this paper sponsored by Committee on Culverts and Hydraulic Structures.